

1
2
3
4
5
6
7
8
9
10
11
12
13
14
15
16
17
18
19
20
21
22
23
24
25
26
27
28
29
30
31
32
33
34
35
36
37
38
39
40
41
42
43
44
45
46
47
48
49
50
51
52
53
54
55
56
57
58
59
60
61
62
63
64
65

Carbonate dissolution in Mesozoic sand- and claystones as a response to CO₂ exposure at 70°C and 20 MPa.

Weibel, R.¹, Kjøller, C.¹, Bateman, K.², Laier, T.¹, Nielsen, L. H.¹, Purser, G.²,

¹ GEUS, Geological Survey of Denmark and Greenland, Øster Voldgade 10, DK-1350 Copenhagen K, Denmark.

² BGS, British Geological Survey, Keyworth, Nottingham, NG12 5GG, United Kingdom.

1
2
3
4
5
6
7
8
9
10
11
12
13
14
15
16
17
18
19
20
21
22
23
24
25
26
27
28
29
30
31
32
33
34
35
36
37
38
39
40
41
42
43
44
45
46
47
48
49
50
51
52
53
54
55
56
57
58
59
60
61
62
63
64
65

Keyword: CO₂ experiments, synthetic pore fluid, *in situ* alterations, reservoir rocks and caprocks, carbonate dissolution, calcite, dolomite, ankerite, siderite, lack of silicate dissolution.

Abstract

The response to CO₂ exposure of a variety of carbonate cemented rocks has been investigated using pressurised batch experiments conducted under simulated reservoir conditions, 70°C and 20 MPa, and with a durations of up to 14 months. Calcite, dolomite, ankerite and siderite cement were present in the unreacted reservoir rocks and caprocks.

Core plugs of the reservoir rocks were used in order to investigate the alterations *in situ*. Crushing of the caprock samples was necessary to maximise reactions within the relatively short duration of the laboratory experiments.

Synthetic brines were constructed for each batch experiment to match the specific formation water composition known from the reservoir and caprock formations in each well. Chemical matched synthetic brines proved crucial in order to avoid reactions due to non-equilibria of the fluids with the rock samples, for example observations of the dissolution of anhydrite, which were not associated with the CO₂ injection, but rather caused by mismatched brines.

Carbonate dissolution as a response to CO₂ injection was confirmed in all batch experiments by both petrographical observations and geochemical changes in the brines. Increased Ca and Mg concentrations after 1 month reaction with CO₂ and crushed caprocks are ascribed to calcite and dolomite dissolution, respectively, though not verified petrographically. Ankerite and possible siderite dissolution in the sandstone plugs are observed petrographically after 7 months reaction with CO₂; and are accompanied by increased Fe and Mn contents in the reacted fluids. Clear evidence for calcite dissolution in sandstone plugs is observed petrographically after 14 months of reaction with CO₂, and is associated with increased amounts of Ca (and Mg) in the reacted fluid. Dolomite in sandstones shows only minor dissolution features, which are not clearly supported by increased Mg content in the reacted fluid.

Silicate dissolution cannot be demonstrated, either by chemical changes in the fluids, as Si and Al concentrations remain below the analytical detection limits, nor by petrographical changes, as partly dissolved feldspar grains and authigenic analcime are present in the sediments prior to the experiments. It is noteworthy, that authigenic K-feldspar and authigenic albite in sandstones show no signs of dissolution and consequently seem to be stable under the experimental conditions.

1
2
3
4
5
6
7
8
9
10
11
12
13
14
15
16
17
18
19
20
21
22
23
24
25
26
27
28
29
30
31
32
33
34
35
36
37
38
39
40
41
42
43
44
45
46
47
48
49
50
51
52
53
54
55
56
57
58
59
60
61
62
63
64
65

1. Introduction

The concentration of carbon dioxide in the atmosphere has increased rapidly in the last 50 years and irreversible climate changes are predicted if the atmospheric carbon dioxide content continues to increase (Ketzer et al. 2009). Subsurface geological storage of CO₂ has been suggested as a possible method for the reduction of CO₂ emissions to the atmosphere. Some geological factors, though, need to be satisfied. Preferably, the geological structure should be closed, the overlying cap rock must hinder vertical migration of CO₂ (Chadwick et al. 2009) and the CO₂-rock interactions within the reservoir rock must not degrade its quality substantially. In Denmark several reservoir rocks exist with potential to be used for CO₂ storage, but none of these reservoir rocks nor their overlying cap rock have been tested experimentally. In order to address this, the most obvious reservoir rocks with different mineralogical compositions (Bunter Sandstone Formation, Skagerrak Formation, Gassum Formation and Halder Sand Formation) and their overlying caprocks (Fjerritslev Formation and Børgelum Formation) have been chosen for investigation of their chemical stability when exposed to CO₂ saturated fluids.

Natural analogue studies and field pilot studies are the most realistic ways of testing the effects of CO₂ storage. However, before field tests can be considered, a reasonable reservoir capability and caprock integrity must be demonstrated. Laboratory experiments supplemented with geochemical modelling are recommended ways of initial assessment (Chadwick et al. 2009). Though codes and databases used for modelling have been refined (e.g. Xu et al. 2004; Ketzer et al. 2009), models still have to be verified experimentally. Laboratory experiments are set up to mimic reservoir conditions, and many experiments have been conducted at or near reservoir pressures and temperatures (e.g. Pearce et al. 1996; Shiraki and Dunn 2000; Bertier et al. 2006; Wigand et al. 2008; Ketzer et al. 2009). Siliciclastic sediments experimentally exposed to CO₂ commonly show the dissolution of carbonate cement and feldspar grains (e.g. Pearce et al. 1996; Shiraki and Dunn 2000; Bertier et al. 2006; Wigand et al. 2009; Ketzer et al. 2009), and feldspar dissolution is supported by observations from natural analogues (e.g. Stevens et al. 2001; Baines and Worden 2004). Clay mineral and carbonate precipitation is documented in some experiments and natural analogues (e.g. Pearce et al. 1996; Shiraki and Dunn 2000; Stevens et al. 2001; Baines and Worden 2004; Bertier et al. 2006; Ketzer et al. 2009).

Together with the temperature and pressure, the ionic strength of the fluid can influence the solubility of CO₂ in water as well as mineral dissolution / precipitation rates (e.g. Weiss 1974; Duan and Sun 2003; Allan et al. 2011), and

1 therefore careful decisions regarding the fluid composition is important for laboratory experiments. Though ionic
2 strength is considered, composition of the formation water has achieved less attention and is to some degree
3 disregarded. Saline brines with different concentrations (c. 10 – 200 g/L total dissolved solids) of NaCl (Pearce et al.
4 1996; Shiraki and Dunn 2000; Wigand et al. 2008) or Na(Ca, Mg, K)Cl (Shiraki and Dunn 2000; Bertier et al. 2006;
5 Ketzer et al. 2009) have been studied experimentally. Despite the findings of Shiraki and Dunn (2000) that anhydrite
6 dissolution occurred only in brine under-saturated with SO_4^{2-} , and not in brines containing SO_4^{2-} , most experiments are
7 performed with simple saline brines of Na(Ca, Mg, K)Cl. In the present experiments synthetic formation brines were
8 used with compositions selected to resemble the *in situ* formation water for each sample (compare Laier 2008). Parallel
9 N_2 experiments were run in order to register mismatched brines and reactions associated with the experimental set up
10 rather than CO_2 exposure, for example corrosion of steel vessels (as described by Bertier et al. 2006). Plugs of the
11 reservoir rocks were used instead of the usual crushed samples in order to enable/facilitate identification of *in situ*
12 alteration phenomena. By taking these precautions we were able to distinguish artefacts related to the experimental
13 setup (or sampling) from actual mineral reaction caused by rock interactions with CO_2 . The purpose of this paper is
14 primarily to investigate the mineral reactions taking place during the CO_2 experiments with duration of up to 14
15 months; and secondarily to identify the possible pitfalls when dealing with laboratory experiments.
16
17
18
19
20
21
22
23
24
25
26
27
28
29
30
31
32
33
34
35
36
37
38
39
40
41
42
43
44
45
46
47
48
49
50
51
52
53
54
55
56
57
58
59
60
61
62
63
64
65

2. Geological background and sediment

mineralogy/petrography

The Danish part of the Norwegian-Danish Basin was formed in Late Carboniferous-Early Permian period by crustal stretching of the area between the stable Fennoscandian Shield and the Ringkøbing-Fyn High consisting of shallow basement highs (Fig. 1). The extension phase was followed by regional subsidence governed by thermal cooling during the Mesozoic. In all, 5-9 km of sandstones, mudstones, evaporates and carbonates were deposited in a wide range of environments (Bertelsen 1980; Nielsen and Japsen 1991; Michelsen et al. 2003). Reservoirs potentially suitable for CO₂ storage are found at several stratigraphic levels. The most important among these are the Lower Triassic Bunter Sandstone Formation, the Triassic Skagerrak Formation, the Upper Triassic-lowermost Jurassic Gassum Formation and the Middle Jurassic Haldager Sand Formation (Fig. 1; Frykman et al. 2009; Mathiesen et al. 2010).

Bunter Sandstone Formation and Skagerrak Formation

The Bunter Sandstone Formation, with up to four regional sandstone units of fluvial and aeolian origin, and interbedded with thick mudstones, is present onshore Denmark in the North German Basin south of the Ringkøbing-Fyn High (Bertelsen 1980; Michelsen and Clausen 2002). Closer towards the northern and eastern margin of the Danish Basin, the well-sorted Bunter Sandstone Formation passes into the poorly-moderately sorted sandstones and mudstones of the Skagerrak Formation (Fig. 1B), which encompasses an up to 2–3 km thick, heterogeneous basin margin succession formed during the Early–Late Triassic (Bertelsen 1980; Nielsen 2003). Both the Bunter Sandstone Formation and the Skagerrak Formation contain mudstones that may act as internal caprocks for the interbedded sandstones, although their sealing capacity has not yet been fully investigated.

The sandstones of the Bunter Sandstone Formation consist mainly of arkoses and subarkoses (Fig. 2; Weibel and Friis 2004). K-feldspar is more common than plagioclase, which is typically more intensively dissolved. Some samples contain numerous ooids; carbonate clasts or clay intraclasts – formed as “rip-up” clasts. The volumetrically important authigenic phases in the Bunter Sandstone Formation are carbonates (calcite and dolomite), anhydrite and clay minerals (illite, chlorite, mixed-layer illite/smectite, mixed-layer smectite/chlorite). Dolomite, calcite and anhydrite may occur as

1 pore-filling cement. Authigenic calcite also occurs as overgrowths on ooids or other carbonate rock fragments and
2
3 dolomite occurs as rhombohedral-shaped single crystals commonly in clay intraclasts. Analcime is present in most
4
5 samples and occurs as perfect, outer crystal shapes, whereas the internal parts frequently have irregular dissolution
6
7 voids. Common subordinate authigenic minerals are feldspar overgrowths, quartz overgrowths, barite, red coatings of
8
9 primarily hematite, anatase and other authigenic opaque minerals (Weibel and Friis, 2004).
10

11
12 The sandstones and conglomerates of the Skagerrak Formation are arkoses, lithic arkoses and subarkoses (Fig. 2;
13
14 Weibel 1998). The feldspar group is completely dominated by K-feldspar, though rare plagioclase grains have been
15
16 identified. Rock fragments are mainly igneous and rarely metamorphic, and in specific geographic areas volcanic rock
17
18 fragments are common. Clay intraclasts, which probably are rip-up clasts from overbank deposits, occur in high
19
20 abundance in few samples. Mica occurs in small amounts in most samples. Transparent and opaque heavy minerals are
21
22 common accessory minerals. The alteration of opaque minerals includes, amongst others, leucoxene replacement of
23
24 ilmenite and hematisation of magnetite, (Weibel 1999; Weibel and Friis 2007). The dominating porosity reducing
25
26 cements in the Skagerrak Formation are carbonates and clays. The clays are dominated by smectite in the shallow wells,
27
28 whereas mixed-layer illite/smectite and illite becomes more abundant with increased burial depth (Weibel 1999). The
29
30 carbonate cement typically consists of dolomite, which occurs as rhombohedral-shaped crystals or as a pore filling
31
32 cement, commonly replacing other mineral phases. Occasionally, the pore filling carbonate cement is calcite or ankerite
33
34 cement instead of dolomite. The red colourations of the shallow buried sandstones (< 2100 m) originate from goethite
35
36 needles, which are pseudomorphously transformed into hematite needles in the deeper buried parts (>2700 m) (Weibel
37
38 1999; Weibel and Groberty 1999). Of minor volumetrically importance are quartz overgrowths, feldspar overgrowths
39
40 and anatase. Anhydrite is a rare late authigenic phase and corrosive to all other mineral phases.
41
42
43
44

45 *Gassum Formation*

46
47 The Gassum Formation is present in most of the Danish area as a 50–300 m thick succession of fluvial and marine
48
49 sandstones interbedded with marine, lagoonal and lacustrine mudstones reflecting repeated fluctuations of sea-level
50
51 during deposition (Nielsen 2003). The formation is overlain by thick marine mudstones of the Fjerritslev Formation
52
53 with large lateral continuity forming a highly competent caprock unit. This probably makes the Gassum Formation one
54
55 of the most promising reservoirs for CO₂ storage in the Danish subsurface.
56
57
58
59
60
61
62
63
64
65

1
2
3 The sandstones of the Gassum Formation are mainly subarkoses and arkoses (Fig. 2; Friis 1987). The feldspar
4 abundance varies across the basin being relatively more abundant in the north-western part than in the eastern part. K-
5 feldspar is more common than albite and Ca-rich plagioclase has not been observed. Alteration of feldspar grains
6 includes partly dissolution, replacement by kaolinite or carbonate, and incipient albitisation at deep burial. Mica, present
7 in all samples, shows varying degrees of alteration from expansion along cleavage planes caused by precipitation of
8 authigenic minerals to compaction along stylolites in the deepest buried parts of the Gassum Formation. Transparent
9 and opaque heavy minerals occur as accessory minerals. The transparent heavy minerals are rutile, zircon and
10 tourmaline, and the opaque minerals are dominated by leucoxene altered ilmenite with adjacent pyrite precipitation
11 (Weibel and Friis 2007). The porosity reduction is mainly due to compaction at burial depths down to 1500 m (Friis
12 1987) and minor changes in the porosity are mainly the result of limited amounts of authigenic phases as siderite, pyrite
13 and calcite besides generation of secondary porosity by feldspar dissolution. At burial depths below 1500 m, the
14 porosity reduction is caused in particular by quartz diagenesis and locally by ankerite cement and kaolinite
15 precipitation. Volumetrically, minor authigenic phases include illite, chlorite and albite.
16
17
18
19
20
21
22
23
24
25
26
27
28
29
30

31 *Haldager Sand Formation*

32
33 The Haldager Sand Formation, dominated by marine and fluvial sandstones, is mainly present in the fault-bounded
34 Sorgenfrei-Tornquist Zone where it locally attains up to 200 m in thickness; outside this zone, it wedges out rapidly
35 toward southwest and northeast (Nielsen 2003). The Haldager Sand Formation is overlain by interbedded marine
36 sandstones and mudstones of the Flyvbjerg Formation and marine mudstones of the Børglum Formation. Toward
37 southwest and west, the Flyvbjerg Formation wedges out and the Haldager Sand Formation is in places directly overlain
38 by marine mudstones of the Børglum Formation, which has a large caprock potential.
39
40
41
42
43
44
45
46
47

48 The sandstones of the Haldager Sand Formation are mainly quartz arenites with subordinate subarkoses (Fig. 2). Quartz
49 dominates the framework grains. K-feldspar is more common than plagioclase, the latter being extremely rare in the
50 deepest wells. Rock fragments are of plutonic, metamorphic or sedimentary origin. Organic matter is abundant in some
51 samples, and occasional root or soil horizons have been reported (Nielsen and Friis 1984; Nielsen 2003). Mica is
52 commonly concentrated in the same samples as the organic matter. Completely kaolinised mica is found in most
53 samples of the Haldager Sand Formation. The authigenic phases is similar to those of the Gassum Formation, however
54
55
56
57
58
59
60
61
62
63
64
65

1 their abundance is typically lower. Early quartz and kaolinite occur randomly distributed in the paralic sandstones,
2
3 whereas calcite cement may be important in the marine deposits (Nielsen and Friis 1984). Siderite, anatase, pyrite and
4
5 alteration products of pyrite like iron-oxide/hydroxides and jarosite are common minor authigenic phases.
6
7
8

9 *Fjerritslev Formation*

10 Fjerritslev Formation is an Early Jurassic thick (up to at least 900 m) relatively uniform succession of marine claystones
11
12 with varying content of silt and sandstone laminae (Pedersen 1986; Michelsen et al. 2003; Nielsen 2003). Depositional
13
14 environment vary from deep offshore central in the Danish Basin to lower shoreface in the Fennoscandian Border zone
15
16 (Pedersen 1985; Michelsen et al 2003; Nielsen 2003). The Fjerritslev Formation is dominated by quartz and relatively
17
18 high amounts of illite and kaolinite, moderate amounts of siderite, minor amounts of calcite, dolomite, chlorite and K-
19
20 feldspar (Table 2).
21
22
23
24

25 *Børglum Formation*

26 Børglum Formation is an Upper Jurassic offshore claystone with varying amounts of silt (Michelsen
27
28 et al. 2003). Thicknesses up to 300 m occur in the centre of the Danish Basin with thinning towards north-east and
29
30 south-west (Michelsen et al. 2003). The Børglum Formation is characterised by relatively high amounts of illite,
31
32 kaolinite and quartz, minor amount of chlorite, smectite, plagioclase and K-feldspar and very low contents of ankerite
33
34 and pyrite (Table 2).
35
36
37
38
39
40
41
42
43
44
45
46
47
48
49
50
51
52
53
54
55
56
57
58
59
60
61
62
63
64
65

3. Methods

3.1. Batch laboratory experiments

All the experiments were performed as batch experiments, using purpose built stainless steel high-pressure reactors, fitted with PTFE liners (Bateman, and Purser, 2010). The batch vessels were fitted with two ports one to maintain gas pressure during the experiments, and the second port fitted with a PEEK dip tube with a filter polypropylene assembly, to allow samples of the fluid to be taken for chemical analysis. Small plug samples were used for the experiments investigating sandstones. This enabled the observation of alterations occurring within the intact sandstones and the description of how alteration gradually penetrates from the rim towards the centre of the plug. For the caprock experiments, the mudstones were carefully crushed and the 250 – 500 µm size fraction used. The caprock samples were crushed as their low porosities were expected to slow the transport of fluid to the mineral surfaces too much for any significant reaction to occur within the duration of the experiments. A quantitative mineralogical composition of the applied sandstone plugs and a semi-quantitative composition of the mudstone samples are presented in Tables 1 and 2. Sandstone plugs and claystone fragments were cleaned in methanol prior to the experiments in order to remove salts from dried out pore fluid.

Assembly of the batch vessels involved first weighing out the sample (core, or crushed sample) into the PTFE liners, followed by the addition of the synthetic formation water. In the experiments using crushed samples a 4:1 water:rock mass ratio was used. Where intact cores were used, an approximate 4:1 water:rock mass ratio was used. A small magnetic stirrer bead was added, and the liner placed into the appropriate steel vessel. The vessels were then placed on top of magnetic stirrers, within an oven (accurate to better than $\pm 0.5^\circ\text{C}$) and connected to the appropriate pressure line. Parallel experiments with an inert gas (N_2) were run simultaneously with the CO_2 experiments in order to provide a ‘base case’ with which to determine which reactions were due to CO_2 reaction and those due to the establishment of fluid/rock equilibrium. The CO_2 and N_2 gases were supplied to the reactors from a pair of ISCO™ syringe pumps running in ‘constant pressure’ mode.

Two batch experiments were conducted for each rock sample, in order to obtain 8 fluid samples taken over a period of 14 months, and to allow the sampling of the reacted solids after both 7 and 14 months reaction. The rock samples were

1 reacted with an appropriate synthetic formation water, with fluid samples taken during one series of batch experiments
2
3 after 1, 3, 5 and 7 months. In the other series of batch experiments, fluid samples were taken after 7, 9, 11 and 14
4
5 months. On termination of each series of batch experiments, after 7 and 14 months, respectively, the reacted rock
6
7 samples were recovered from the vessels, and cleaned in isopropyl alcohol, in order to minimise 'salting out' of the
8
9 brines before being analysed. The experiments were undertaken close to reservoir conditions with a temperature of
10
11 70°C and at a pressure of 20 MPa, using synthetic formation water (Table 3). The composition of the synthetic pore
12
13 fluids was based on chemistry of the formation water either from the same wells as the core material or if not available
14
15 from a nearby well (Table 3).
16
17
18
19

20 **3.2. Analytical methods**

21
22 The experimental fluids sampled from the batch vessels were analysed for major and some minor cations (Si, Al, Fe, Sr,
23
24 Ba, Co, Ni, Cu, Zn, Cr, Mo, Cd, P, Pb, V, Li, B, As, Se and total S) using inductively coupled plasma - optical emission
25
26 spectroscopy (ICP-OES), and for major and some minor anions (F^- , Br^- , Cl^- , NO_3^- , HPO_4^{2-}) using ion chromatography
27
28 (IC). SO_4^{2-} was calculated from total S under the assumption that all sulphur occurred as sulphate. Analysis of HCO_3^-
29
30 was performed by titration against sulphuric acid. Measurements of pH were made on cooled, depressurised samples at
31
32 room temperature, using an Orion® 900A pH meter calibrated using Whatman® NBS traceable buffers at pH 4, 7 and
33
34 10.
35
36
37

38 Petrography was evaluated from transmitted light and reflected light microscopy of polished thin sections. Modal
39
40 compositions of the sandstones were obtained by point counting minimum 500 points in each thin section, excluding the
41
42 porosity. The thin sections were etched and stained for K-feldspar. Supplementary studies of crystal morphologies,
43
44 dissolution features and paragenetic relationships were performed on gold coated rock chips mounted on stubs and on
45
46 carbon coated thin sections using a Phillips XL 40 scanning electron microscope (SEM). The scanning electron
47
48 microscope was equipped with secondary electron detector (SE), back-scatter detector (BSE); and with a Thermo
49
50 Nanotrace 30 mm² detector surface window and a Pioneer Voyager 2.7 10 mm² window Si(Li) detector energy
51
52 dispersive X-ray analysis (EDX) system. The electron beam was generated by a tungsten filament operating at 17 kV
53
54 and 50-70 µA. Potential risks during the experiment are leaks, evaporation and drying of the top of the plug as more
55
56 fluid samples are removed. Therefore, petrographical investigations were preferentially undertaken of the bottom-part,
57
58
59
60
61
62
63
64
65

1 outermost part of the plugs. Recognition of intensified dissolution on already partly dissolved detrital grains and partly
2 dissolved authigenic phases is somewhat subjective.
3

4
5
6
7 Chemical composition of the carbonates was undertaken using a JEOL JXA-8200 Microprobe working at 15kV and
8
9 12μA and the smallest possible beam size (5μm) for siderite, ankerite and dolomite, whereas a larger beam size (~ 10
10 μm) was used when measuring calcite.
11
12

13
14
15 Bulk samples for X-ray diffraction analysis (XRD) were mounted with random orientation. Samples were scanned on
16
17 an automated Philips© PW 3710 X-ray diffractometer with automatic divergence slit, using graphite monochromated
18
19 CuKα radiation. Quantification of major mineral phases based on bulk samples was done by Rietveld analysis of X-ray
20
21 diffractograms.
22
23

24
25 The samples were crushed manually and dispersed ultrasonically in distilled water. The fraction >30 μm was removed
26
27 by sedimentation and the 2-30 μm by centrifugation in a centrifugal particle size analyser using the method described
28
29 by Slater & Cohen (1962). The suspensions were flocculated in 1 M NaCl and following this excess salt was removed
30
31 by centrifugation and washing with water and ethanol. Oriented specimens were prepared by pipette of the < 2 μm clay
32
33 fraction, which were either Mg-saturated, K-saturated, Mg-saturated and ethylene glycolated or K-saturated and heated
34
35 for an hour at 300°C. The clay specimens were analysed by a Phillips 1050 X-ray diffractometer with pulse-height
36
37 selection and β-filtered Co-Kα. The discrete minerals were identified from peak positions on the XRD diffractograms.
38
39

40
41
42 The porosity and permeability were measured according to the API RP-40 standard (API 1998). Gas permeability was
43
44 measured at a confining pressure ~ 2.8 MPa (400 psi), and at a mean N₂ gas pressure of ~ 1.5 bar (bar absolute) = 0.15
45
46 MPa (permeabilities below 0.05 mD was measured using a bubble flowmeter). He-porosity was measured unconfined.
47
48
49
50
51
52
53
54
55
56
57
58
59
60
61
62
63
64
65

4. Results

4.1. Fluid chemistry evolution during experiments

The changes in fluid composition during the batch experiments are shown for the chemical parameters expected to vary due to the CO₂ addition (HCO₃⁻, Mn, Ca, Mg, Fe_{TOTAL}, SO₄²⁻, K) (Figs 3 and 4).

The significant increase in HCO₃⁻ concentration in CO₂ experiments during the first month was accompanied by an increase in concentration of most major ions, Ca, Mg, Mn, Na K and SO₄²⁻ (assuming that the total sulphur measured by ICP exists as sulphate), in Figs 3 and 4. The concentration of the major ions even increase within the first month for the N₂ batches, which were intended as 'blank' control experiments. This illustrates that even though the initial composition of the synthetic pore fluid was carefully designed to represent formation water ('reservoir estimate' in Table 3 is indicated as 'target' on Figs 3 and 4), some degree of disequilibrium exists at the beginning of the experiments. The reacted fluid composition quickly approaches equilibrium, probably within the first 1000 minutes (e.g. Pokrovsky et al 2009; Schott et al. 2009) and the rapid far-from equilibrium reactions are not represented in the experiments.

Afterwards, slower overall mineral reactions take place as indicated by the less pronounced increase in ion concentrations during the remaining part of the experiments. Si and Al concentrations are not shown as the concentration of these two species remain below detection limits (0.75 mg/l for Si and 0.1 mg/l for Al) in most samples measured. The exception is the samples from the experiments with the Gassum Formation from the Stenlille-18 well.

Discarding the increase in concentration during the first month, the most pronounced changes in reacted fluids in the CO₂ experiments when compared with the N₂ experiments are:

- Increased Ca concentration (Bunter Sandstone and Fjerritslev formations; Figs 3 and 4),
- Increased Mn concentration (Skagerrak, Gassum, Haldager Sand, Børglum and Fjerritslev formations; Figs 3 and 4),
- Increased Fe concentration followed by a drop in Fe concentration (Skagerrak, Gassum, Haldager Sand, Børglum Formations; Figs 3 and 4),
- Increased Mg concentration (Børglum Formation; Fig. 4),
- Increased K concentration (Børglum Formation; Fig. 4).

1 The most pronounced changes in each experiment are summarised in Table 4. Increased $[\text{SO}_4^{2-}]$ (measured as total-S) is
2
3 observed in the N_2 experiment of Bunter Sandstone, Gassum and Børglum formations.
4
5
6

7 A gradual increase in concentration of the expected conservative elements (Br^- and Cl^-) may be due to either minor
8
9 evaporation or other experimental uncertainties. Consequently, the general increase in the major ions during the
10
11 experiments may in addition to the mineral reactions with CO_2 , reflect uncertainties that are related to the experimental
12
13 set-up and/or the measurements of the fluid samples.
14
15
16
17
18
19

20 **4.2. Petrographically observed mineral reaction during experiments**

21
22

23 The advantage of applying sandstone plugs in the reservoir rock experiments rather than crushed samples is that it
24
25 eliminates artefacts caused by the crushing process, so that more definite conclusions on the mineral alterations can be
26
27 made from the petrographical analyses. Furthermore, the porosity and permeability could be measured both prior to and
28
29 after the experiments. However, the use of plugs has made it important to concentrate observations close to the rim
30
31 rather than in the more central parts of the plugs; i.e. as even in the 14 month duration experiments, the reactions cannot
32
33 be found in the centre of the plugs. The draw-back of using the plugs is that the reactions are much slower compared to
34
35 crushed samples and that the transport of fresh unreacted brine may be the limiting factor for reaction. However, the
36
37 identification of mineral alteration by petrographical analysis, in the caprock samples is hampered by the crushing
38
39 process as well as the fine-grained nature of the caprocks.
40
41
42

43 The most pronounced mineral alterations in the CO_2 experiments, when compared with the N_2 experiments, are:
44

- 45 • Dissolution of calcite (Bunter Sandstone Formation; Fig. 5),
- 46
- 47 • Dissolution of ankerite (Gassum and Skagerrak formations; Fig. 5),
- 48
- 49 • Dissolution of dolomite (Børglum and Bunter Sandstone formation; Fig. 5),
- 50
- 51 • Possible dissolution of siderite (Gassum Formation; Fig. 5),
- 52
- 53 • No identified dissolution features on authigenic albite (Gassum and Skagerrak formations; Fig. 6),
- 54
- 55 • No identified dissolution features on authigenic K-feldspar (Bunter Sandstone Formation; Fig. 6).
- 56
- 57

58 Dissolution of anhydrite (Bunter Sandstone Formation) is equally common in N_2 and CO_2 experiments.
59
60
61
62
63
64
65

1
2
3 4.2.1. *Bunter Sandstone Formation*
4

5 The plugs of the Bunter Sandstone Formation show incipient corrosion of calcite rhombs after 7 months of CO₂
6 experiment and clear signs of calcite cement dissolution after 14 months of experiments (Figs 5C and 5D). The calcite
7 cement has a low content of trace elements (Table 5). Possible corrosion features on dolomite rhombs appear after 14
8 months. The Bunter Sandstone Formation contains partly dissolved feldspars and authigenic analcime with internal
9 dissolution voids prior to the experiments. Based solely on the petrographical analysis, it is not possible to verify an
10 increased degree of dissolution of these minerals during the experiment. Authigenic K-feldspar seems to be unaffected
11 in both experiments (Figs 6E and 6F). Dissolution of anhydrite is observed in both the CO₂ and the N₂ pressurised
12 experiments.
13
14
15
16
17
18
19
20
21
22

23 4.2.2. *Skagerrak Formation*
24

25 The Skagerrak Formation plugs show clear signs of ankerite dissolution after both 7 and 14 months of CO₂ exposure
26 (Figs 5A and 5B). The ankerite cement has a high Ca, Fe, Mg and low Mn content (Table 5). Partly dissolved detrital
27 feldspar grains occur in the Skagerrak Formation, but an increased degree of dissolution of detrital feldspar cannot be
28 confirmed petrographically (Figs 6A and 6B).. Authigenic albite shows no trace of corrosion (Figs 6C and 6D).
29
30
31
32
33
34
35
36

37 4.2.3. *Gassum Formation*
38

39 The Gassum Formation (Vedsted-1 well) plug shows clear signs of dissolution of ankerite cement after both 7 and 14
40 months of CO₂ exposure. The ankerite cement has a high content of Ca, Fe, Mg and a low content of Mn (Table 5).
41 Siderite rhombs are partly dissolved in both the CO₂ and the N₂ experiments (Figs 5E and 5F). The siderite dissolution
42 features in the N₂ experiments are of a peculiar character, which may be due to problems during thin section
43 preparation. Siderite has typically a low Mn content (Table 5). Partly dissolved detrital K-feldspar and plagioclase are
44 commonly observed both in the unreacted and reacted samples, whereas authigenic albite shows no corrosion features.
45 A small colour change of the plugs is common in most experiments e.g. from whitish grey to yellowish grey. However,
46 the plug from the Gassum Formation in the Vedsted-1 well changes its colour from whitish grey to orange during the
47 CO₂ experiment, but not during the N₂ experiment.
48
49
50
51
52
53
54
55
56
57
58
59
60
61
62
63
64
65

1 The experiments with the Gassum Formation sample from the Stenlille-18 well were found to contain infiltrated drilling
2 mud (consisting of smectitic clay, barite and calcite). This complicates the comparison of alterations in the solid rock
3 samples with reacted fluid changes during the experiments. Partial dissolution of both detrital K-feldspar and
4 plagioclase prior to and after the experiments is common. Siderite and calcite rhombs are rare constituents in the
5 Gassum Formation in the Stenlille-18 well, partial dissolution of these due to CO₂ exposure cannot be verified by
6 petrographical analysis. Euhedral pyrite occurs with etched surfaces after 7 months of experiment, whereas changes in
7 the pyrite framboids are difficult to recognise. Gypsum is a common constituent prior to the cleaning in methanol of the
8 plugs; some remnants may have survived.

21 4.2.4. *Haldager Sand Formation*

22 The Haldager Sand Formation contains abundant pyrite framboids with alteration rims of iron-oxide/hydroxides or
23 jarosite. An increased degree of dissolution of pyrite alteration rims seems to occur in the CO₂ experiments and maybe
24 also the N₂ experiments. The mineralogical composition of the dissolved alteration product cannot be verified
25 petrographically; though the liberation of SO₄²⁻ suggests sulphate dissolution (e.g. gypsum, jarosite). Siderite has been
26 observed previously in other samples examined from the Haldager Sand Formation (Weibel et al. 2010), but has not
27 been positively identified in plugs used in this work.

39 4.2.5. *Caprocks*

40 The Fjerritslev Formation sample contains only small amounts of calcite, dolomite and siderite rhombs, though without
41 clear signs of incipient dissolution. Dolomite appears with clear dissolution features after the CO₂ experiments in the
42 Børglum Formation sample (Figs 5G and 5H).

4.3. Porosity and permeability changes during experiments

The sandstones porosities are unchanged or higher after the CO₂ experiments when the samples are cleaned in methanol (Fig. 7). Sandstone permeability is also higher after the CO₂ experiments, though it has not been possible to measure permeability for all experimental plugs.

5. Discussion

The parallel CO₂ and N₂ experiments have ensured that identification of mineral changes related to mineral interaction with CO₂ can be distinguished from changes occurring due to the experimental setup. This way, we hope to emphasize the conclusions that can be drawn from the experiments as well as to discuss the pitfalls that may accompany experimental results.

5.1. Carbonate reactions

Carbonate dissolution is the most prominent reaction observed in the CO₂ pressurised experiments. Ankerite dissolution (Skagerrak and Gassum formations) is observed petrographically in the CO₂ experiments and is supported by observed increased Fe and Mn concentrations in the reacted fluids (Figs 3,5A and 5B). In addition, the ratio between Fe and Mn in the reacted fluids (Fe:Mn ~ 5:1) compares reasonably well to the measured composition of ankerite in the Gassum and Skagerrak formations (Table 5). The changes in aqueous Ca and Mg concentrations, due to ankerite dissolution, are too low to be detected given the relatively high initial content of these two ions in the initial fluids. Thus, using the ankerite composition of Table 5 and the observed Fe concentration of 3 mmol/L in the CO₂ batch from the Gassum experiment, one would expect an increase in Ca concentration of approximately 10 mmol/L which is less than 2% of the initial Ca concentration, and as such is lower than the 5% uncertainty related to the analytical measurement. Siderite (Gassum Formation) appears with two different types of dissolution features in the CO₂ and N₂ experiments, that may have different origins, i.e. mineral reaction with CO₂ and/or sample preparation (Figs 5E and 5F). Siderite is subordinate to ankerite and therefore its dissolution does not affect the reacted fluid Fe:Mn ratio considerably (Fig. 3). Calcite dissolution (Bunter Sandstone Formation and Fjerritslev Formation) during CO₂ experiments is petrographically documented (Bunter Sandstone Formation) and supported by increased amounts of Ca in the reacted fluids (Figs 3, 5C and 5D). Incipient dissolution of dolomite rhombs (Bunter Sandstone and Børglum formations) could explain corrosion features and liberation of especially Mg and to a smaller extent Fe and Mn in the reacted fluid during the CO₂ experiment (Fig. 3, Table 5).

1 Based on the petrographical observations, dissolution of siderite was observed in the 7-month duration CO₂ experiments
2
3 (though some minor alteration may also have occurred in the N₂ experiments). Intense dissolution of ankerite occurred
4
5 over both 7- and 14-months of CO₂ exposure. Incipient calcite dissolution was visible after 7-months of reaction but
6
7 more intense dissolution features were observed after 14 months of reaction. Incipient dissolution of dolomite could be
8
9 recognised only after 14 months of experiment. The petrographically based 'apparent sequence' of carbonate reaction
10
11 rates when exposed to CO₂, beginning with dissolution of siderite and ankerite, then calcite and ending with dolomite is
12
13 supported by the results of Bertier et al. (2006), who found that Fe-rich parts of carbonate cement were least stable in
14
15 CO₂ experiments. The lower dissolution rate of dolomite compared to calcite dissolution rates is in agreement with
16
17 experimental findings both without and with the presence of CO₂ (e.g. Chou et al. 1989; Palandri and Kharaka 2004;
18
19 Pokrovsky et al. 2009; Schott et al. 2009). However, the apparent overall sequence of dissolution rates observed in our
20
21 experiments is more likely to reflect that the dissolution rate of carbonates in the experiments is limited by diffusion of
22
23 fresh unreacted brine into the plug rather than the chemical reaction rate at the surface of the minerals. Thus, if only
24
25 surface reactions were taken into account, dissolution of calcite prior to ankerite and siderite would be expected, as the
26
27 reaction order for surface-controlled dissolution of divalent metal carbonates is Mg<Fe<Mn<Ca (Pokrovsky and Schott
28
29 2002). Similarly, the siderite dissolution rate (R: 1.8·10⁻¹¹ mol/cm²s; Golubev et al. 2009) is in kinetic experiments at
30
31 25°C and pH: 4 under the influence of CO₂ lower than the rate of dolomite dissolution (R: 3.2·10⁻¹⁰ mol/cm²s; Chou et
32
33 al 1989). Judging from the measured aqueous chemistry, the major dissolution of carbonates takes place within the first
34
35 month of the experiments (Fig. 3), which is also in good agreement with the reaction rates observed in single mineral
36
37 dissolution experiments (Golubev et al. 2009). Quantitative estimates on the carbonate dissolution rates in the sediments
38
39 applied in our study would require more frequently fluid sampling in the early phase of the experiments than has been
40
41 the case in these experiments.
42
43
44

45 Carbonate dissolution would expect to result in a minor increase in porosity of the samples as a result of the reaction
46
47 with CO₂ during experiments. The possible porosity change can be calculated from the observed difference in aqueous
48
49 concentrations between the CO₂ experiments and the reference N₂ experiments and by assuming that the prominent
50
51 carbonate dissolution occurring in each formation is that observed from the petrographical studies (cf. Table 4). E.g.,
52
53 the difference in Fe concentration of approximately 1.6 mmol/L between the parallel CO₂ and N₂ experiments with the
54
55 Skagerrak Formation can be assumed to stem from the dissolution of ankerite (Table 6). The corresponding change in
56
57 porosity can be estimated to be in the order of 0.2% (Table 6). In general, the calculated porosity changes that may
58
59
60
61
62
63
64
65

1 occur due to carbonate dissolution are small and range between 0.1-0.7. %. The calculated porosity changes correspond
2
3 very well with the actually measured porosity changes in samples characterised by ankerite dissolution (Gassum
4
5 Formation in the Vedsted-1 well and Skagerrak Formations), suggesting that in these samples, the major cause for
6
7 porosity change may be the dissolution of carbonate. For other samples (Bunter Sandstone Formation, Gassum
8
9 Formation in the Stenlille-18 well and Haldager Sand Formation), the estimated porosity change from the difference in
10
11 aqueous chemistry is somewhat less than the measured porosity change, which may be partly due to dissolution of other
12
13 minerals than carbonate and partly due to disintegration of the rocks and grain loss, making an accurate porosity
14
15 measurement after experiments difficult. Similarly, the poor condition of samples after experiments hampered
16
17 permeability measurements of all samples after experiments. However, for samples where permeability could be
18
19 measured, the general increase in porosity seems to be associated with a corresponding increase in permeability (Fig. 7).
20
21
22

23 As demonstrated by the petrographical analysis, carbonate dissolution features occur primarily in the outer rim of the
24
25 sandstone plugs. Dissolved CO₂, assuming the kinetics of CO₂ dissolution is faster than minerals dissolution rates
26
27 (Allan et al. 2011), penetrates through the pore system in the sandstone plug and dissolution occurs where the fluid is in
28
29 direct contact with carbonate cement. Complete dissolution does not take place in sandstone plugs over the 14 month-
30
31 duration of the experiments. Crushing of the samples increases the surface area available for reaction and increases the
32
33 likelihood of collision between dissolved CO₂ and carbonate minerals. Increased surface area in crushed caprock sample
34
35 (Børglum Formation) explains the more pronounced dissolution of dolomite compared to the sandstone plug (Bunter
36
37 Sandstone Formation). Diffusion rates of solutes into and out of the pores in the sandstone plugs limit the extent of the
38
39 water-rock interaction. The difference between reaction rates in powdered samples, which is usually applied in
40
41 laboratory experiments, compared with plug samples has important implications for forward modelling. Likely, an even
42
43 larger difference exists between sandstone plugs exposed to agitated synthetic reacted fluid in batch experiments
44
45 compared to reservoir sandstones with even more limited formation water convection. Thus, in geological settings the
46
47 carbonate dissolution is likely to be even slower than observed in these long term (14 month) experiments.
48
49
50
51
52
53
54
55
56
57
58
59
60
61
62
63
64
65

5.2. Silicate reactions

Silicate dissolution cannot be confirmed with any certainty from the experiments. Both Si and Al concentrations in the reacted fluids remain below the analytical detection limits and give no indication of silicate dissolution.

Petrographically, it is not possible to verify an increased degree of dissolution of albite (Bunter Sandstone Formation), K-feldspar (Skagerrak and Gassum Formation) and analcime (Bunter Sandstone Formation), but it cannot be excluded. However, authigenic K-feldspar (Bunter Sandstone Formation) and authigenic albite (Skagerrak and Gassum formations) seem to remain unaffected in the CO₂ experiments, and thus we infer this as evidence for a high degree of feldspar stability during experiments. This is different from observations of feldspar dissolution seen in other CO₂ experiments (Pearce et al. 1996; Shiraki and Dunn 2000; Wigand et al. 2008; Ketzer et al. 2009).

Carbonate dissolution rates of $\sim 2 \times 10^{-10}$ mol/cm²s (Jordan and Rammensee, 1998) exceed those of aluminosilicates $\sim 10^{-19} - 10^{-15}$ mol/cm²s (Allan et al. 2011). If no carbonate minerals are present to provide pH buffering, aluminosilicates will start to dissolve. Experiments with sandstone of low carbonate content (Haldager Sand Formation) result in lower pH than other experiments, but still the Al and Si concentrations in the reacted fluids remain below the detection limits for the analytical methodology used. Sulphates are possibly dissolved in this experiment and in such a case silicate reactions may be subdued until less stable phases are dissolved. Prolonged CO₂ experiments could have a more clear effect on the silicates, as the use of sandstone plugs as opposed to crushed samples may have retarded the extent of some of the reactions.

5.3. Influence of experimental design on observations

5.3.1. Mineral reactions due to mismatched pore fluid composition

Several experiments conducted to examine the effect of CO₂ exposure on reservoir rocks have been performed with a synthetic pore fluid containing only NaCl, or combinations of Na(Ca, Mg, K)Cl (Pearce et al. 1996; Bertier et al. 2006; Wigand et al. 2008) and even de-ionised water (Pearce et al. 1996; Ketzer et al. 2009). Consequently in those experiments, there is a risk of dissolution being caused simply due to the pore fluid being under saturated with respect to the minerals present. The influence of pore fluid composition has been considered only in few experiments (e.g. Shiraki and Dunn 2000). In our experiments, we have aimed at using synthetic brines that were chemically comparable to the natural brines of the various formations.

Dissolution of anhydrite is from a petrographical point of view equally intensive in both the CO₂ and the N₂ experiments conducted with samples of the Bunter Sandstone Formation. This suggests that the initial sulphate content in the synthetic pore fluids was too low. If the sulphate concentration of the initial fluid had been closer to the natural content, then anhydrite dissolution would probably not have occurred, as documented by Shiraki and Dunn (2000). Observations of anhydrite dissolution occurring in long-term (15 months) CO₂ experiments with solutions consisting of (Na, Mg, Ca, K)Cl (Fischer et al. 2010), de-ionised water, and synthetic seawater (Pearce et al. 1996) may consequently be a result of the under saturation with respect to sulphate.

Pore fluid changes during one N₂ pressurised experiments (Gassum Formation in the Stenlille-18 well) are characterised by increased sulphate content, which does not seem to have a straightforward petrographical explanation.

Sulphide/sulphate may originate from fines migration of barite present in the drilling mud, from remnants of gypsum due to insufficient cleaning in methanol or the result of pyrite corrosion. The most likely explanation is dissolution of remnants of gypsum as neither Fe nor Ba accompany the sulphate increase. Incomplete cleaning of caprocks may also result in local occurrences of gypsum (Børglum Formation), which reveals the inherent heterogeneity of the claystones.

1
2
3
4
5
6
7
8
9
10
11
12
13
14
15
16
17
18
19
20
21
22
23
24
25
26
27
28
29
30
31
32
33
34
35
36
37
38
39
40
41
42
43
44
45
46
47
48
49
50
51
52
53
54
55
56
57
58
59
60
61
62
63
64
65

5.4.1. Reactions related to the experimental set up

Contamination of the plugs from the Gassum Formation (Stenille-18 well) with drilling mud may have lead to the presence of highly reactive mineral phases, such as smectite and calcite, as well as barite. Consequently, the presence of Al₂O₃ and SiO₂ concentrations above the detection limits, seen in these experiments may reflect reaction with these contaminant phases.

The decrease in Fe concentration in the last fluid samples taken from the Skagerrak Formation in CO₂ experiments (Fig. 3) may be due to precipitation of iron-oxide/hydroxides during the experiments. The oxidation of iron necessary for the iron-oxide/hydroxide precipitation may be due to a leak in the pressure vessel during the experiment though this has not been verified.

6. Conclusion

A variety of carbonate cements, calcite, ankerite, siderite and dolomite, are represented in the investigated sandstones (Bunter Sandstone, Skagerrak, Gassum and Haldager Sand formations) and two claystones, which are potential caprocks (Børglum and Fjerritslev formations). Carbonate dissolution is the most prominent response to the presence of CO₂ in the experiments conducted at 70°C and 20 MPa with durations up to 14 months. Petrographical investigations indicate that the degree of dissolution varies according to the chemical composition of the carbonate cement. Ankerite cement (Skagerrak and Gassum formations) dissolution is observed petrographically after only 7 months of reaction, and this is supported by changes in the pore fluid chemistry. Possible corrosion of siderite (Gassum Formation) occurs after 14 months of reaction. Clear signs of calcite cement dissolution (Bunter Sandstone Formation) are observed in samples after 14 months reaction, and this is supported by increased Ca concentrations in the reacted fluid. Possible corrosion features on dolomite rhombs (Bunter Sandstone and Børglum formations) are recognised after 14 months of experiments. Dolomite dissolution, in the Børglum Formation is supported by increased Mg concentrations in the synthetic reacted fluids.

Our investigations emphasize the importance of having more than one feature indicating the same process, i.e. dissolution features and increased concentrations of associated elements in the reacted fluid samples. Carbonate dissolution features are accompanied by increased dissolved concentrations of Fe, Mn, Mg and Ca depending on the carbonate chemistry. Silicate dissolution cannot be confirmed in the experiments. Si and Al in the reacted fluids remain below detection limits and consequently fluid chemistry alone does not support silicate dissolution. Silicate dissolution of detrital feldspar grains and authigenic analcime had occurred prior to the experiments, and an increase in dissolution due to the exposure to CO₂ can therefore not be verified, nor rejected petrographically. However, authigenic K-feldspar and authigenic albite show no signs of corrosion.

The experiments also demonstrate the importance of using pore fluid with a chemical composition appropriate to the core sample. The larger the gap between the real and synthetic pore fluid compositions, the higher the risk of causing dissolution, which relates solely to the experimental setup rather than reaction with CO₂. The use of inert (with N₂ gas)

1 experiments, conducted in this study, running simultaneously with the CO₂ experiments has proven to be valuable for
2
3 such a comparison.
4
5
6
7
8
9
10

11 **7. Acknowledgement**

12

13
14
15
16
17
18 The work presented in the paper is part of the outcome of the Aqua-DK research project supported by the Danish EUDP
19 programme, and the authors would like to acknowledge the funding by the Energy Agency and financial support by
20 Vattenfall and DONG Energy. General petrographical investigations of the sandstone formations were supported by a
21 grant from The Danish Council for Strategic Research. The paper is published with the permission of the Geological
22 Survey of Denmark and Greenland (GEUS), and with the permission of the Executive Director, BGS (NERC). Thanks
23 to Executive Editor Prof. Michael Kersten and two anonymous referees for their helpful comments which considerably
24 improved an earlier draft.
25
26
27
28
29
30
31
32
33
34
35
36
37
38
39
40
41
42
43
44
45
46
47
48
49
50
51
52
53
54
55
56
57
58
59
60
61
62
63
64
65

8. References

- Allan, M. M., Turner, A., Yardley, B. W. D. 2011. Relation between dissolution rates of single minerals and reservoir rocks in acidified pore waters. *Applied Geochemistry* 26, 1289–1301.
- API, 1998: API RP 40, Recommended Practice for Core Analysis, second edition, American Petroleum Institute, Washington DC.
- Baines, S. J., Worden, R. H. 2004. The long-term fate of CO₂ in the subsurface: natural analogues for CO₂ storage. In: Baines, S. J. and Worden, R. H. (eds.), *Geological storage of carbon dioxide*. Geological Society of London, Special Publication 233, 59–85.
- Bateman, K, Purser, G,. 2010. Geological storage of CO₂ in the Danish Underground: Evaluation of the Response of the Reservoir and Cap Rocks to CO₂ storage. British Geological Survey External Report, CR/10/153. 37pp.
- Bertelsen, F. 1980. Lithostratigraphy and depositional history of the Danish Triassic. *Danmarks geologiske Undersøgelser B 4*, 59 pp.
- Bertier, P., Swennen, B., Laenen, B., Lagrou, D., Dreesen, R. 2006. Experimental identification of CO₂-water-rock interactions caused by sequestration of CO₂ in Westphalian and Buntsandstein sandstones of the Campine Basin (NE-Belgium). *Journal of Geochemical Exploration* 89, 10–14.
- Chadwick, A., Arts, R., Bernstone, C., May, F., Thibeau, S., Zweigel, P. 2008. Best practice for the storage of CO₂ in saline aquifers. British Geological Survey Occasional Publication 14, 267p.
- Duan, Z., Sun, R. 2003. An improved model calculating CO₂ solubility in pure water and aqueous NaCl solutions from 273 to 533 K and from 0 to 2000 bar. *Chemical Geology* 193, 257–271.

- 1 Fine, S. 1986. The diagenesis of the Lower Triassic Bunter Sandstone Formation, Onshore Denmark. Geological
2 Survey of Denmark, A 15.
3
4
5
6
7 Fischer, S., Liebscher, A., Wandrey, M. and the CO₂ SINK Group. 2010. CO₂-brine-rock interaction – First results of
8 long-term exposure experiments at in situ P – T conditions of the Ketzin CO₂ reservoir. *Chemie der Erde* 70, 155–
9 164.
10
11
12
13
14
15 Friis, H. 1987. Diagenesis of the Gassum Formation Rhaetian-Lower Jurassic, Danish Subbasin. Geological Survey of
16 Denmark A 18, 41pp.
17
18
19
20
21 Frykman, P., Nielsen, L.H., Vangkilde-Petersen, T., Anthonsen, K. 2009: The potential for large-scale, subsurface
22 geological CO₂ storage in Denmark. In: Bennike, O., Garde, A.A., Watt, W.S. (eds.) Review of Survey activities
23 2008. Geological Survey of Denmark and Greenland Bulletin 17, 13–16.
24
25
26
27
28
29 Golubev, S. V, Bénézeth, P., Schott, J., Dandurand, J. L., Castillo, A. 2009. Siderite dissolution kinetics in acidic
30 aqueous solutions from 25 to 100°C and 0 to 50 atm pCO₂. *Chemical Geology* 265, 13–19.
31
32
33
34
35 Ketzer, J. M., Iglesias, R., Einloft, S., Dullius, J., Ligabue, R., de Lima, V. 2009. Water-rock-CO₂ interactions in saline
36 aquifers aimed for carbon dioxide storage: Experimental and numerical modelling studies of the Rio Bonito
37 Formation (Permian), southern Brazil. *Applied Geochemistry* 24, 760–767.
38
39
40
41
42
43 Laier T. 2008. Chemistry of Danish saline formation waters relevant for core fluid experiments- Fluid chemistry data
44 for lab experiments related to CO₂ storage on deep aquifers. Geological Survey of Denmark and Greenland Report
45 2008/48, 10p.
46
47
48
49
50
51
52
53
54
55
56
57
58
59
60
61
62
63
64
65

- 1 Mathiesen, A., Kristensen, L. Bidstrup, T., Nielsen, L. H. 2009. Vurdering af det geotermiske potentiale i Danmark (in
2 Danish). Danmark og Grønlands Geologiske Undersøgelse Rapport 2009/59, 30p.
3
4
5
6
7 Mathiesen, A., Nielsen, L.H., Bidstrup, T. 2010. Identification of the potential geothermal reservoirs in Denmark.
8 Geological Survey of Denmark and Greenland Bulletin 20, 19-22.
9
10
11
12
13 McBride, E. F. 1963. A classification of common sandstones. *Journal of Sedimentary Petrology* 33, 664-669.
14
15
16
17
18 Michelsen, O., Clausen, O.R. 2002. Detailed stratigraphic subdivision and regional correlation of the southern Danish
19 Triassic succession. *Marine and Petroleum Geology* 19, 563-587.
20
21
22
23
24 Michelsen, O., Nielsen, L.H., Johannessen, P., Andsbjerg, J., Surlyk, F. 2003. Jurassic Lithostratigraphy and
25 stratigraphic development onshore and offshore Denmark. In: Ineson, J. R. and Surlyk, F. (eds): *The Jurassic of*
26 *Denmark and Greenland*. Geological Survey of Denmark and Greenland Bulletin 1, 147–216.
27
28
29
30
31
32 Nielsen, L.H. 2003. Late Triassic – Jurassic development of the Danish Basin and Fennoscandian Border Zone,
33 Southern Scandinavia. In: Ineson, J. R. and Surlyk, F. (eds): *The Jurassic of Denmark and Greenland*. Geological
34 Survey of Denmark and Greenland Bulletin 1, 459–526.
35
36
37
38
39
40 Nielsen, B. L., Friis, H. 1984. Diagenesis of Middle Jurassic Haldager Formation Sandstone in the Danish Subbasin,
41 North Jutland. *Bulletin of the Geological Society of Denmark* 33, 273–285.
42
43
44
45
46 Nielsen, L.H., Japsen, P., 1991. Deep wells in Denmark 1935-1990. Lithostratigraphic subdivision. *Danmarks*
47 *geologiske Undersøgelser A* 31, 179 pp.
48
49
50
51
52 Palandri, J. L. and Kharaka, Y. K. 2004. A compilation of rate parameters of water-minerals interaction kinetics for
53 application to geochemical modelling. U. S. Geological Survey, Open file report 2004-1068, 64p.
54
55
56
57
58
59
60
61
62
63
64
65

- 1 Pearce, J. M., Holloway, S., Wacker, H., Nelis, M. K., Rochelle, C., Bateman, K. 1996. Natural occurrences as
2 analogues for the geological disposal of carbon dioxide. *Energy Convers. Mgmt* 37, 1123–1128.
3
4
5
6
7 Pedersen, G. 1985. Thin, fine-grained storm layers in muddy shelf sequence: an example from Lower Jurassic in the
8 Stenlille 1 well, Denmark. *Journal of the Geological Society (London)* 142, 357 – 374.
9
10
11
12
13 Pokrovsky, O. S. and Schott, J. 2002. Surface chemistry and dissolution kinetics of divalent metal carbonates.
14 *Environmental Science Technology* 36, 426-432.
15
16
17
18
19 Pokrovsky, O. S., Golubev, S. V., Schott, J., Castillo, A. 2009. Calcite, dolomite and magnesite dissolution kinetics in
20 aqueous solutions at acid to circumneutral pH, 25 to 150°C and 1 to 55 atm $p\text{CO}_2$: New constraints on CO_2
21 sequestration in sedimentary basins. *Chemical Geology* 265, 20-32.
22
23
24
25
26
27 Schott, J., Pokrovsky, O. S., Oelkers, E. H. 2009. The link between mineral dissolution/precipitation kinetics and
28 solution chemistry. *Reviews in Mineralogy and Geochemistry* 70, 207-258.
29
30
31
32
33
34 Sbai, M. A., Azaroual, M. 2011. Numerical modeling of formation damage by two-phase particulate transport processes
35 during CO_2 injection in deep heterogeneous porous media. *Advances in Water Resources* 34, 62-82.
36
37
38
39
40 Schott, J., Pokrovsky, O. S., Oelkers, E. H. 2009. The link between mineral dissolution/precipitation kinetics and
41 solution chemistry. *Reviews in Mineralogy and Geochemistry* 70, 207-258.
42
43
44
45
46 Shiraki, R., Dunn, T. L. 2000. Experimental study on water-rock interactions during CO_2 flooding in the Ten sleep
47 Formation, Wyoming, USA. *Applied Geochemistry* 15, 265-279.
48
49
50
51
52 Slater, C., Cohen, L. 1962. A centrifugal particle analyser. *Journal of Scientific Instruments* 39, 614–617.
53
54
55
56
57
58
59
60
61
62
63
64
65

- 1 Stevens, S. H., Pearce, J. M., Rig, A., A., J. 2001. Natural analogues for geological storage of CO₂: An integrated global
2
3 research program. First National Conference on Carbon Sequestration, U.S. Department of Energy. National
4
5 Energy Technology Laboratory, May 15-17, 2001, Washington, D. C., 12p.
6
7
8
- 9 Weibel, R. 1998. Diagenesis in oxidising and locally reducing conditions – an example from the Triassic Skagerrak
10
11 Formation, Denmark. *Sedimentary Geology* 121, 259–276.
12
13
14
- 15 Weibel, R. 1999. Effects of burial on the clay assemblages in the Triassic Skagerrak Formation, Denmark. *Clay*
16
17 *Minerals* 34, 619–635.
18
19
20
- 21 Weibel, R., Groberty, B. 1999. Pseudomorphous transformation of goethite needles into hematite in sediments of the
22
23 Triassic Skagerrak Formation, Denmark. *Clay Minerals* 34, 657–661.
24
25
26
- 27 Weibel, R., Friis, H. 2004. Opaque minerals as keys for distinguishing oxidising and reducing diagenetic conditions in
28
29 the Lower Triassic Bunter Sandstone, North German Basin. *Sedimentary Geology* 169, 129–149.
30
31
32
- 33 Weibel, and Friis, H. 2007. Alteration of opaque heavy minerals as reflection of geochemical conditions in depositional
34
35 and diagenetic environments. In: Mange, M. A. and Wright, D. T. (eds.) *Heavy minerals in use. Developments in*
36
37 *Sedimentology*, Elsevier 58, 305–333.
38
39
40
- 41 Weibel, R., Olivarius, M., Nielsen, L. H., Abramovitz, T., Kjølner, C. 2010. Petrography and diagenesis of the Triassic
42
43 and Jurassic sandstones, eastern part of the Norwegian-Danish Basin. Danmarks. Danmarks og Grønlands
44
45 *Geologiske Undersøgelser*, Report 2010/114, 83p.
46
47
48
- 49 Weiss, R.F. (1974), Carbon dioxide in water and seawater: The solubility of a non-ideal gas. *Marine Chemistry* 2, 203–
50
51 215.
52
53
54
55
- 56 Wigand, M, Carey, J. W. Schütt, H., Spangenberg, E., Erzinger, J. 2008. Geochemical effects of CO₂ sequestration in
57
58 sandstones under simulated in situ conditions of deep saline aquifers. *Applied Geochemistry* 23, 2735–2745.
59
60
61
62
63
64
65

1
2
3
4
5
6
7
8
9
10
11
12
13
14
15
16
17
18
19
20
21
22
23
24
25
26
27
28
29
30
31
32
33
34
35
36
37
38
39
40
41
42
43
44
45
46
47
48
49
50
51
52
53
54
55
56
57
58
59
60
61
62
63
64
65

Xu, T., Apps, J. A., Preuss, K. 2004. Numerical simulation of CO₂ disposal by mineral trapping in deep aquifers.
Applied Geochemistry 19, 917 – 936.

1
2
3
4
5
6
7
8
9
10
11
12
13
14
15
16
17
18
19
20
21
22
23
24
25
26
27
28
29
30
31
32
33
34
35
36
37
38
39
40
41
42
43
44
45
46
47
48
49
50
51
52
53
54
55
56
57
58
59
60
61
62
63
64
65

Figure captions

Figure 1

A. Map of Denmark showing the regional potential for CO₂ storage in the Triassic-Jurassic formations. Modified after Mathiesen et al. (2009) and Frykmann et al. (2009). B. Stratigraphic scheme simplified after Michelsen and Clausen (2002) and Nielsen (2003).

Figure 2

Traditional classification of sandstones according to McBride (1963).

Figure 3

Evolution of the fluid chemistry during CO₂ experiment and inert experiment with N₂ for the reservoir sandstones.

Figure 4

Evolution of the fluid chemistry during CO₂ experiment and inert experiment with N₂ for the caprocks.

Figure 5

Carbonate dissolution features in reservoir rocks and caprocks in CO₂ experiment compared with carbonate appearance in the inert N₂ experiment. A and B. Ankerite cement (An) with no dissolution features in N₂ experiment (7 months) and with dissolution along crystal faces, after CO₂ experiment (7 months), BSC images. Skagerrak Formation in the Vedsted-1 well, 2064.87m. C and D. Calcite cement (Ca) with no signs of dissolution after N₂ experiment (14 months) and with clear sign of dissolution after CO₂ experiment (14 months), BSC images. Bunter Sandstone Formation in the Tønder-4 well, depth 1663.27m. E and F. Siderite rhombs (Si) with some alteration after N₂ experiment (14 months) and with typical dissolution features after CO₂ experiment (14 months), BSC images. Gassum Formation in the Vedsted-1 well, depth 2010.1m. G and H. Dolomite (Do) crystals showing no sign of dissolution after N₂ experiment (14 months) possible incipient dissolution after CO₂ experiment (14 months), SEM images. Børglum Formation in the Haldager-1 well, 1041 m.

1
2
3
4
5
6
7
8
9
10
11
12
13
14
15
16
17
18
19
20
21
22
23
24
25
26
27
28
29
30
31
32
33
34
35
36
37
38
39
40
41
42
43
44
45
46
47
48
49
50
51
52
53
54
55
56
57
58
59
60
61
62
63
64
65

Figure 6

Silicate appearance after CO₂ experiment and after the inert experiment with N₂. A and B. Partly dissolved K-feldspar (K-f) with relatively unaffected albite lamellae (Al), prior to experiment and after CO₂ experiment (7 months), BSC images. Skagerrak Formation in the Vedsted-1 well, 2064.87m. C and D. Authigenic albite with no sign of dissolution after N₂ experiment (14 months) and after CO₂ experiment (14 months), SE images. Skagerrak Formation in the Vedsted-1 well, 2064.87m. E and F. K-feldspar overgrowth (K-fo) with no signs of dissolution after N₂ experiment (14 months) and after CO₂ experiment (14 months), SE images. Bunter Sandstone Formation in the Tønder-4 well, depth 1663.27m.

Figure 7

Porosity (A) and permeability (B) prior to experiments versus after experiment values.

Table 1

Modal composition obtained by point counting of the applied sandstone plugs, prior to experiments.

Table 2

Bulk rock mineral composition of the applied mudstones based on Rietveld analysis of X-ray diffractographs.

Table 3

Estimated composition of pore fluids in the Danish reservoir sandstones versus synthetic pore fluids applied in the experiments.

Table 4

Overview of prominent mineral and fluid changes during CO₂ and N₂ batch experiments.

1
2
3
4
5
6
7
8
9
10
11
12
13
14
15
16
17
18
19
20
21
22
23
24
25
26
27
28
29
30
31
32
33
34
35
36
37
38
39
40
41
42
43
44
45
46
47
48
49
50
51
52
53
54
55
56
57
58
59
60
61
62
63
64
65

Table 5

Chemical composition of carbonates investigated by microprobe analysis.

Table 6

Porosity changes in CO₂ experiments calculated based on differences in aqueous concentrations between CO₂ and N₂ experiments as well as from He-porosimetry measurements prior to and after experiments. The estimated amount of carbonate dissolved varies between formations and probably reflect that both aqueous concentrations as well as the estimate on the initial carbonate content are connected with some degree of uncertainty.

Table 1

Formation	Bunter Sandstone	Skagerrak	Gassum	Gassum	Haldager Sand
Depth (m)	1663.27	2064.87	2010.12	1663.44	1155.5
Well	Tønder-4	Vedsted-1	Vedsted-1	Stenlille-18	Vedsted-1
Samples ID		VE1-Sk206487	VE1-Ga201012	ST18-Ga166344	VE1-Ha115550
DETRITAL					
Quartz	29.8	67.2	59.4	84.2	82.0
K-feldspar	16.8	8.4	6.8	0.6	8.0
Plagioclase	6.6	5.6	9.6	0.8	0.6
Mica	5.4	0.4	1.4	0.0	0.6
Intraclasts + allogenic clays	6.2	0.0	0.2	9.8	4.4
Sedi. Rock fragments	6.4	0.4	1.2	0.2	0.2
Metamorphic rock fragm.	0.0	0.0	0.8	0.0	0.2
Volcanic rock fragments	0.2	0.2	0.0	0.0	0.0
Plutonic rock fragm.	4.4	0.8	2.0	1.2	0.6
Transparent heavy min.	0.8	0.0	0.8	0.2	0.4
Opaque	3.4	0.2	0.4	0.6	0.2
AUTHIGENIC PHASES					
Quartz	0.0	5.2	2.0	1.0	0.8
Feldspar	0.0	0.0	0.0	0.0	0.0
Calcite	3.4	0.0	1.0	0.6	0.0
Dolomite / ankerite	0.0	3.2	2.4	0.0	0.0
Siderite	0.0	0.0	0.4	0.0	0.0
Anhydrite	1.4	0.0	0.0	0.0	0.0
Barite	0.0	0.6	0.2	0.0	0.0
Analcime	2.2	0.0	0.0	0.0	0.8
Red coatings	9.0	0.0	0.0	0.0	0.0
Pyrite	0.0	0.0	0.6	0.0	0.2
Anatase	0.0	0.0	0.8	0.0	0.0
Infiltration clay	0.0	0.0	0.0	0.2	0.0
Smectite	0.0	0.0	0.0	0.0	0.0
Illitic and chloritic clays	3.6	1.8	6.0	0.0	0.4
Kaolin	0.4	6.0	4.0	0.6	0.6
TOTAL	100.0	100.0	100.0	100.0	100.0

Table 2

Formation Well	Quartz	K-feldspar	Albite	Ankerite	Dolomite	Calcite	Siderite	Anhydrite	Analcime	Pyrite	Kaolinite	Chlorite	Illite / muscovite	Smectite	Gypsum
	%	%	%	%	%	%	%	%	%	%	%	%	%	%	%
Børglum Haldager-1	33	4	5		2						27	3	23	1	1
Fjerritslev Stenlille-1	30	1	Tr		2	3	12				18	2	25	Tr	

Note that all values < 5 % are liable to high uncertainty. Tr = trace of the mineral.

Table 3

Formation		Bunter Sandstone		Skagerrak		Gassum		Gassum		Haldager Sand		Børglum		Fjerritslev	
Well		Tønder-4		Vedsted-1		Vedsted-1		Stenlille-18		Vedsted-1		Haldager-1		Stenlille-1	
		Formation water		Formation water		Formation water		Formation water		Formation water		Formation water		Formation water	
		Synthetic	Sample data from	Synthetic	Sample data from	Synthetic	Sample data from	Synthetic	Sample data from	Synthetic	Sample data from	Synthetic	Sample data from	Synthetic	Sample data from
Formation			Bunter S.		Skagerrak		Skagerrak		Gassum		Gassum		Haldager		Fjerritslev
Well			Tønder-5		Thisted-2		Thisted-2		Stenille-19		Thisted-2		Haldager-1		Stenlille-1
GEUS Fluid	No.	6		7*		2*		1		3		4		5	
Starting	ml	160		160		120		160		120		60		60	
Vessel	No.	BGS035		BGS038		BGS034		BGS031		BGS039		BGS021		BGS024	
	Type	NEW		OLD		NEW		OLD		OLD		OLD		OLD	
Gas		CO ₂		CO ₂		CO ₂		CO ₂		CO ₂		CO ₂		CO ₂	
pH		6.19		6.59	6.6	6.59	6.6	6.21	6.2	6.44	6.4	5.70		6.17	6.4
Ca ²⁺	mg/l	2879	9500	16985	23500	16985	23500	9980	11500	6371	7500	7360	8110	4986	5700
Mg ²⁺	mg/l	1526	1900	2458	3340	2458	3340	1356	1600	1252	1500	1368	1550	1184	1400
Na ⁺	mg/l	100595	115000	52004	70000	52004	70000	51202	59000	48035	55000	41768	46000	51421	58000
K ⁺	mg/l	1492	1700	1432	1880	1432	1880	976	1100	226	250	233	240	309	290
HCO ₃ ⁻	mg/l	5.00		5.00	30	5.00	30	5.00	80	5.00	43	5.00		5.00	61
Cl ⁻	mg/l	154429	200000	137268	166000	137268	166000	100768	113000	90285	102000	79748	90000	91264	103000
SO ₄ ²⁻	mg/l	345	500	339	290	339	290	877	15	349	10	360	50	464	15
Br ⁻	mg/l	1313	1500	841	980	841	980	359	440	269	290	272	300	279	310
Sr	mg/l	0.83		569	620	569	620	561	660	326	380	437	500	514	600
Total Fe	mg/l	2.46		21.6	30	21.6	30	47.6	60	33.5	40	4.25		24.6	30
Si ⁴⁺	mg/l	bdl		bdl		bdl		bdl		bdl		bdl		bdl	
Al		bdl		bdl		bdl		bdl		bdl		bdl		bdl	

* Pore fluids 2 and 7 are similar. Bdl = below detection limit. DST#3 = drill stem test

Table 4

Formation	Reactions due to CO ₂ exposure		Reactions in N ₂ experiment		Artefacts
	Fluid changes	Mineral alterations	Fluid changes	Mineral alterations	
Bunter Sandstone	Increase in HCO ₃ ⁻ Increase in Ca Increase in Mg?	Calcite dissolution Dolomite corrosion possible	Increase in SO ₄ ⁻	Anhydrite dissolution	Anhydrite dissolution
Skagerrak	Increase in HCO ₃ ⁻ Increase in Fe Increase in Mn	Ankerite dissolution			
Gassum (Vedsted-1 well)	Increase in HCO ₃ ⁻ Increase in Mn Initial increase in Fe, then drop	Ankerite dissolution Siderite dissolution	Drop in Fe at the end of experiment	Reddish coating (iron-oxide/hydroxide) on all grains	Oxidation and precipitation of iron-oxide/hydroxides
Gassum (Stenlille-18 well)	Increase in HCO ₃ ⁻ Increase in Fe Increase in Mn Increase in Ca?	Siderite dissolution? Calcite dissolution?	Increase in SO ₄ ⁻		Drilling mud reactions (or fines migration?) Dissolution of gypsum?
Haldager Sand	Increase in HCO ₃ ⁻ Increase in Fe Increase in Mn Increase in SO ₄ ⁻	Dissolution of jarosite?	Increase in SO ₄ ⁻		
Fjerritslev	Increase in HCO ₃ ⁻ Increase in Fe Increase in Mn Increase in Ca	Calcite dissolution			
Børglum	Increase in HCO ₃ ⁻ Increase in Mg Increase in Fe Increase in Mn Increase in K	Dolomite dissolution Cation exchange of the smectite/illite or incipient K-feldspar dissolution?	Increase in SO ₄ ⁻		Dissolution of gypsum possible (Gypsum occurs in some samples, even though cleaned in methanol)

Table 5

Carbonate phase	Formation	FeCO₃	CaCO₃	MgCO₃	MnCO₃	SUM
Calcite	Bunter Sandstone	0.44	96.78	0.89	0.28	98.38
Dolomite	Bunter Sandstone	0.52	53.82	37.45	1.77	93.57
Ankerite	Skagerrak	18.81	53.32	17.62	3.04	92.84
Ankerite	Gassum (Vedsted-1 well)	18.05	54.79	18.51	2.42	93.84
Siderite	Gassum (Vedsted-1 well)	73.32	2.54	5.31	2.84	84.07
Siderite	Gassum (Stenlille-1 well)	82.70	0.90	0.75	0.11	84.52

Table

Formation	Carbonate with identified dissolution ¹⁾	Water chemistry indicator ²⁾	Δ Conc. (mmol/L)	Mineral density (g/cm ³)	Mole mass (g/mol) ³⁾	Δ Vol. (cm ³)	Δ Porosity Calc (%) ⁴⁾	Δ Porosity Meas. (%) ⁵⁾
Bunter Sandstone	Calcite	Ca	10	2.71	100.1	0.038	0.5	3.4 ⁶⁾
Skagerrak	Ankerite	Fe	1.6	2.93	100.8	0.024	0.2	0.2
		Mn	0.15			0.014	0.1	
Gassum (Vedsted-1)	Ankerite	Fe	3	2.93	100.8	0.055	0.7	0.9
		Mn	0.2			0.023	0.3	
	Siderite	Fe	3	3.00	111.2	0.015	0.2	
		Mn	0.2			0.015	0.2	
Gassum (Stenlille-18)	Siderite	Fe	2	3.00	115.0	0.008	0.1	1.4 ⁷⁾
		Mn	N/A			N/A	N/A	
Haldager Sand	N/A	N/A	N/A	N/A	N/A	N/A	N/A	0.9

1) Excess dissolution observed in CO₂ batch reactors (cf. Table 4)

2) Increased concentration in water from CO₂ batch compared to N₂ batch

3) Calculated based on Table 5

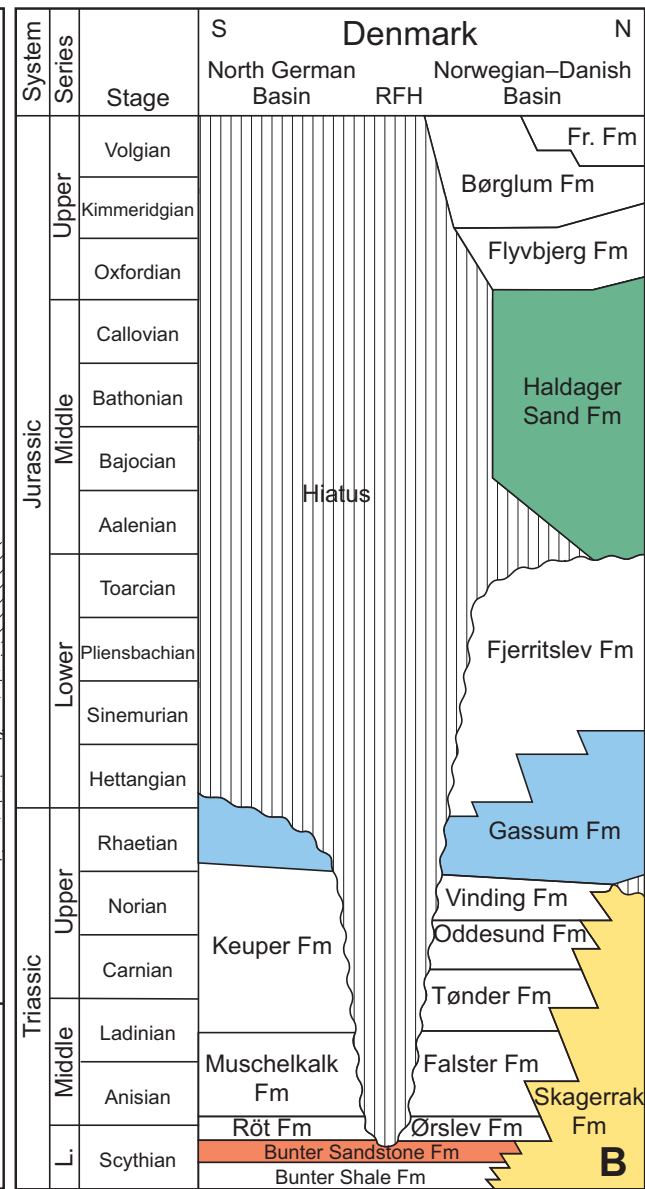
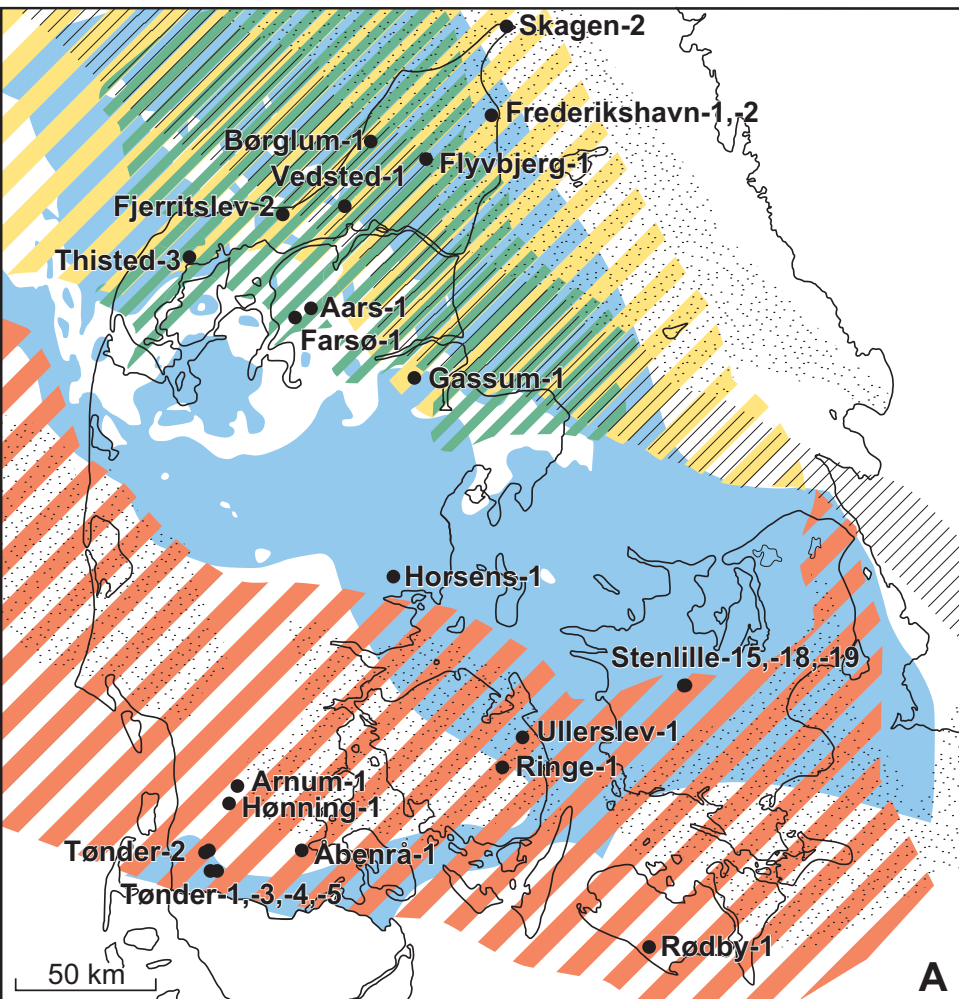
4) Calculated porosity change stemming from the estimated dissolved mass/volume of the specific mineral

5) Measured porosity change during experiments – influenced by fines loss during experiments and cleaning

6) Comparably high due to anhydrite dissolution

7) Comparably high due to dissolution and fines migration of drilling mud

Figure



B

Figure 2

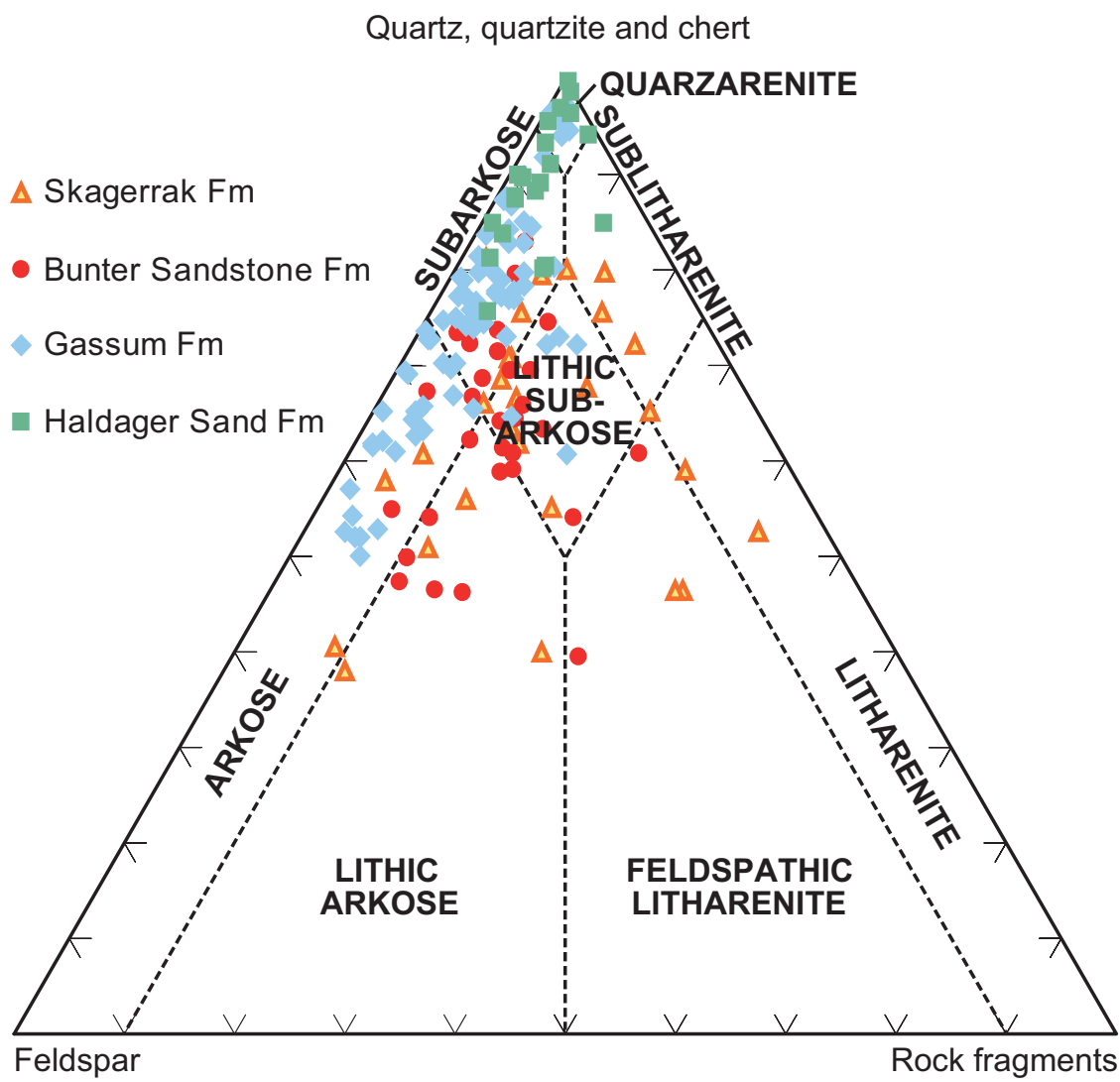
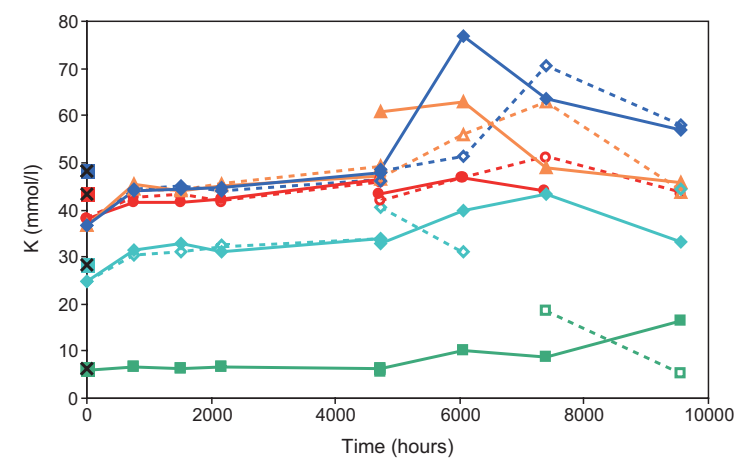
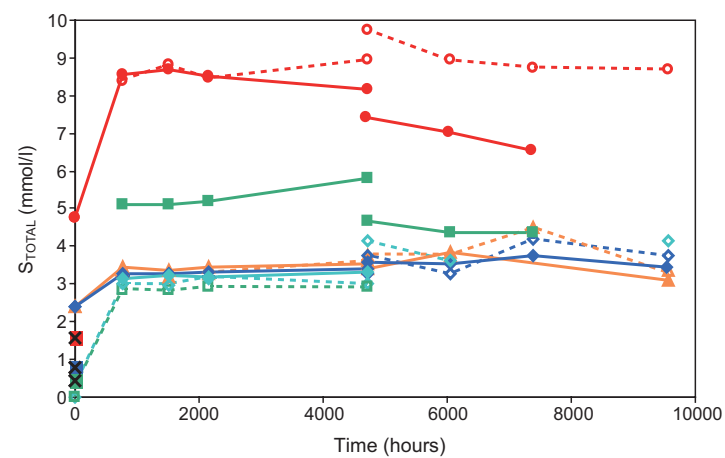
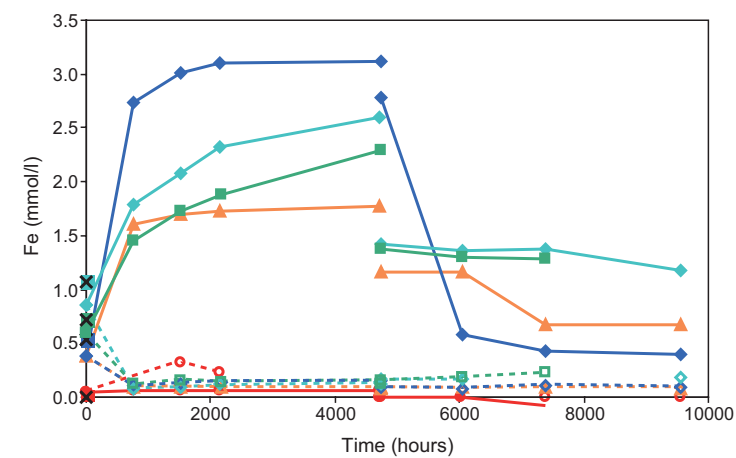
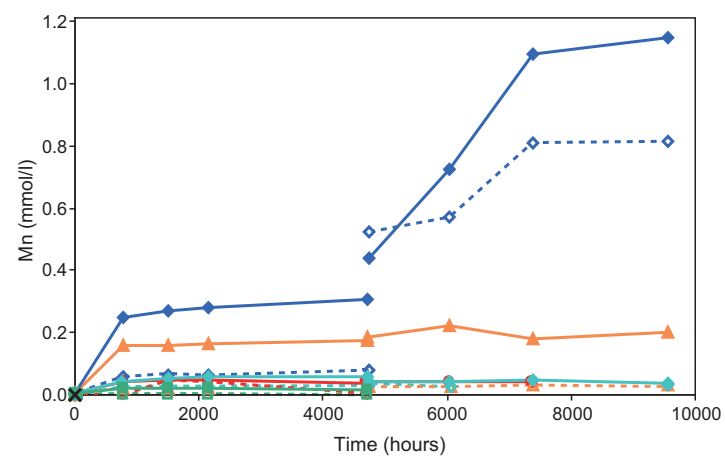
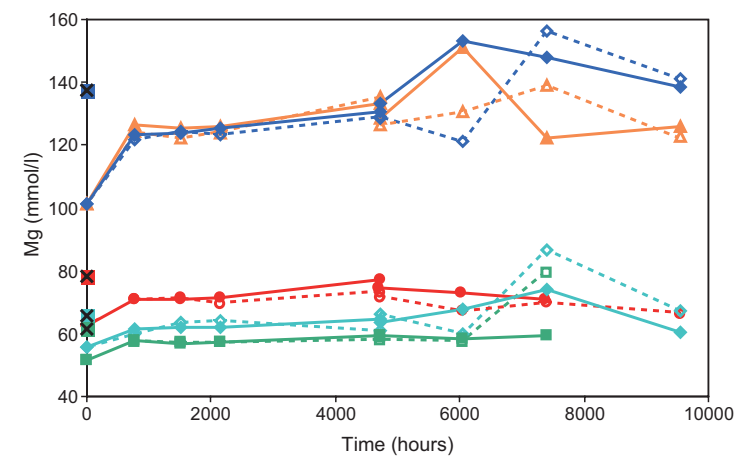
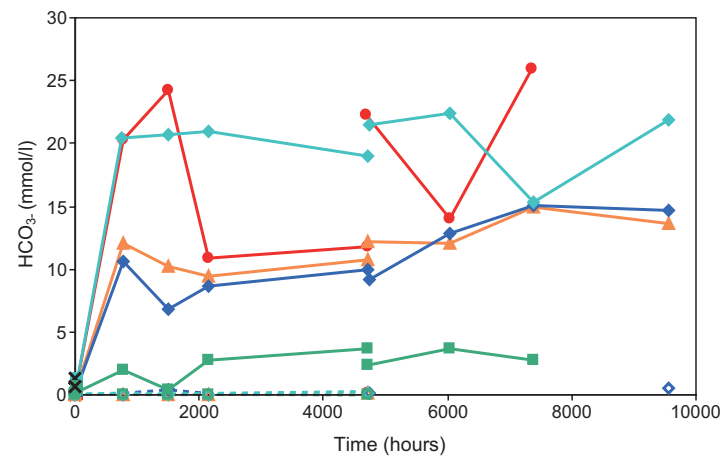
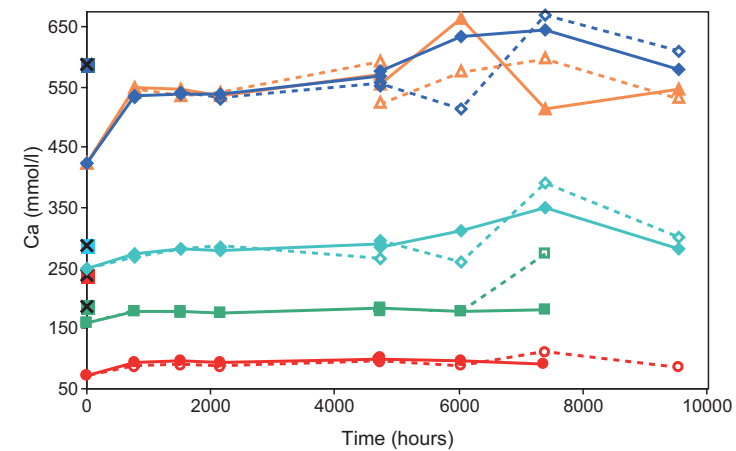
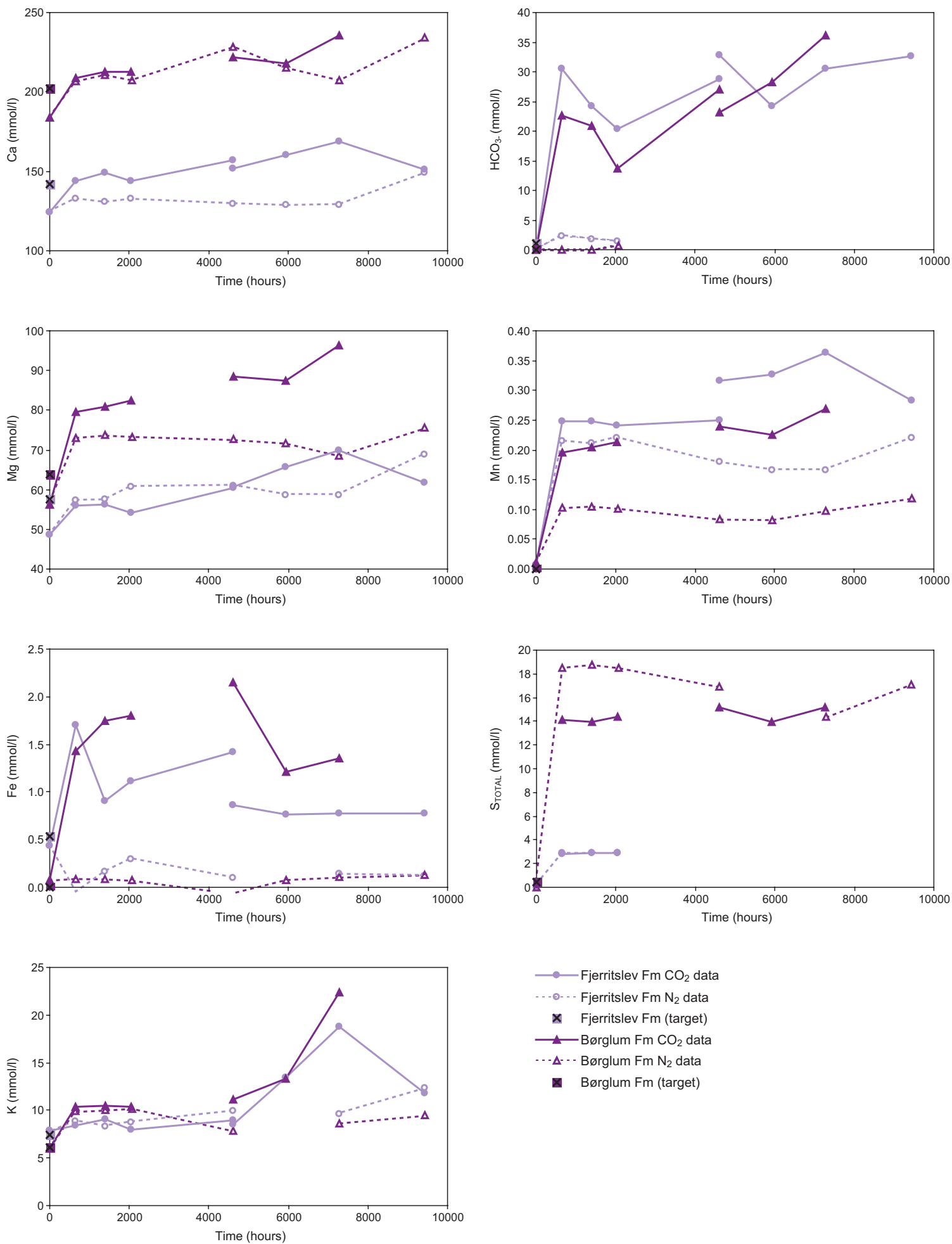


Figure 3



- Bunter Sandstone Fm CO₂ data
- - -○- - - Bunter Sandstone Fm N₂ data
- Bunter Sandstone Fm (target)
- ▲— Skagerrak Fm CO₂ data
- - -△- - - Skagerrak Fm N₂ data
- Skagerrak Fm (target)
- ◆— Gassum Fm (Vedsted-1) CO₂ data
- - -◇- - - Gassum Fm (Vedsted-1) N₂ data
- Gassum Fm (Vedsted-1) (target)
- ◆— Gassum Fm (Stenlille-18) CO₂ data
- - -◇- - - Gassum Fm (Stenlille-18) N₂ data
- Gassum Fm (Stenlille-18) (target)
- Haldager Sand Fm CO₂ data
- - -□- - - Haldager Sand Fm N₂ data
- Haldager Sand Fm (target)

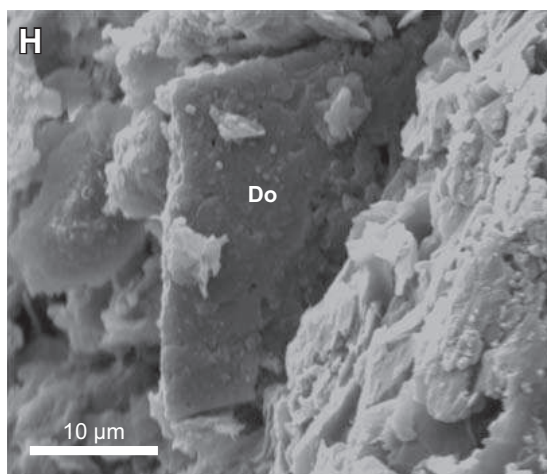
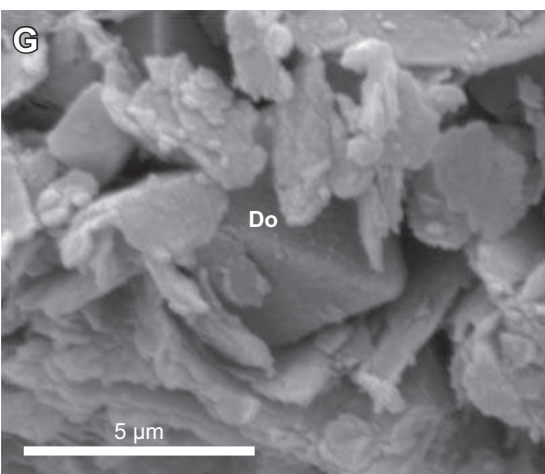
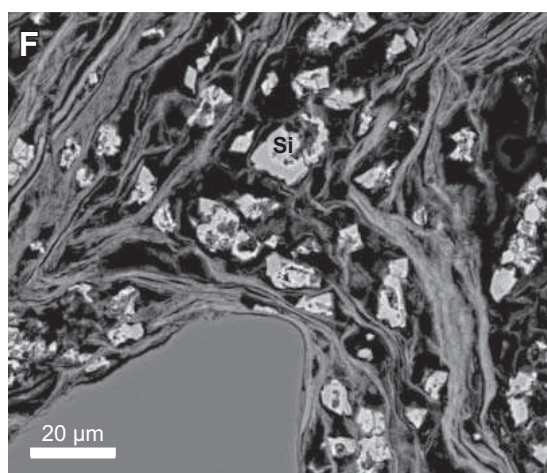
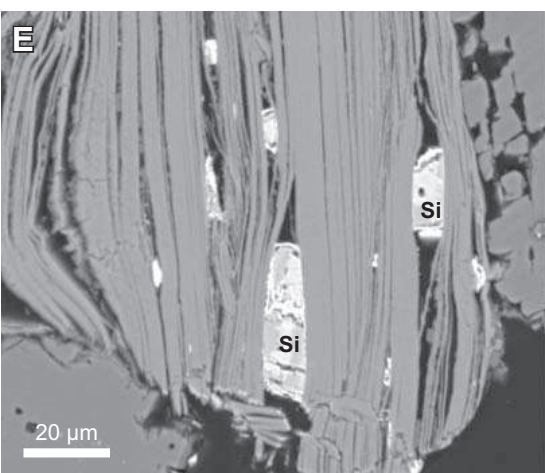
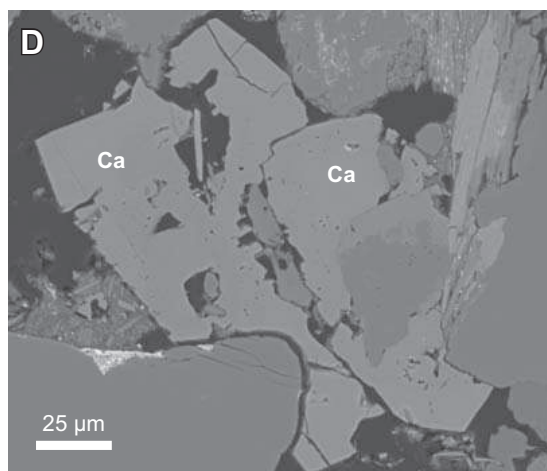
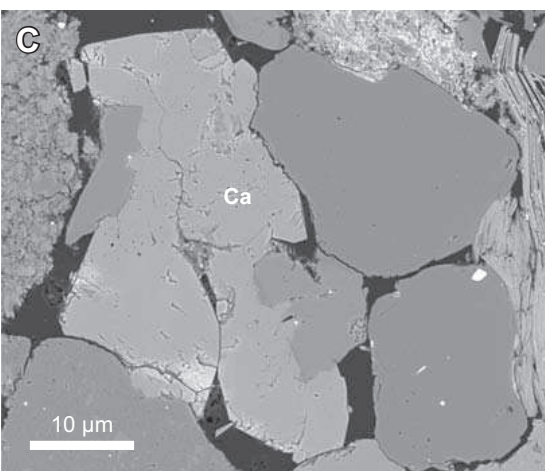
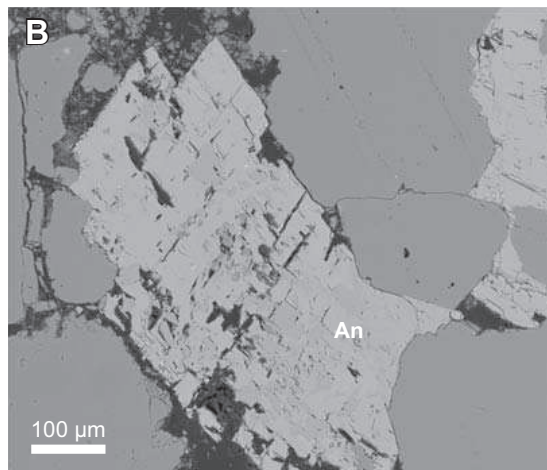
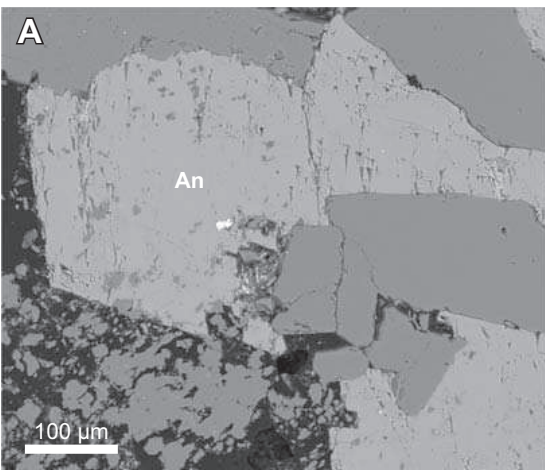
Figure 4

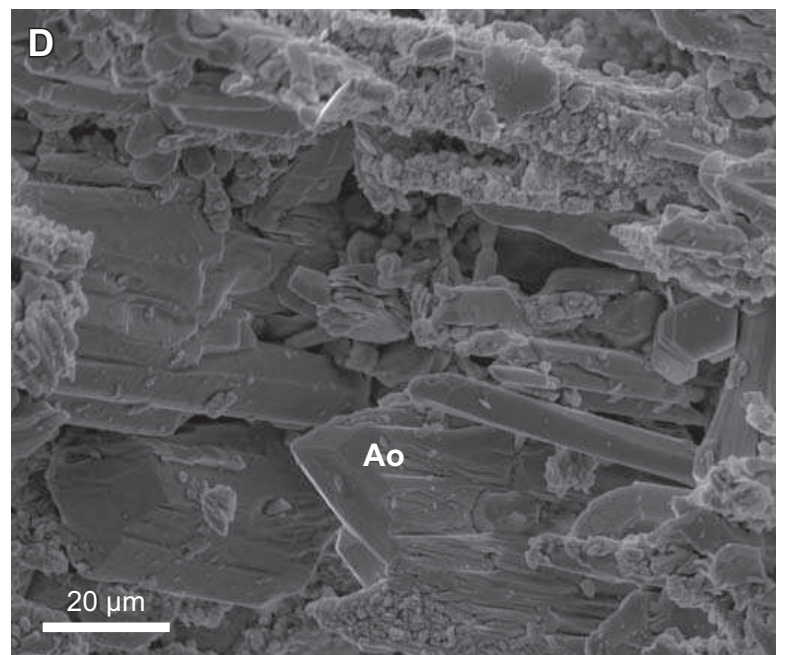
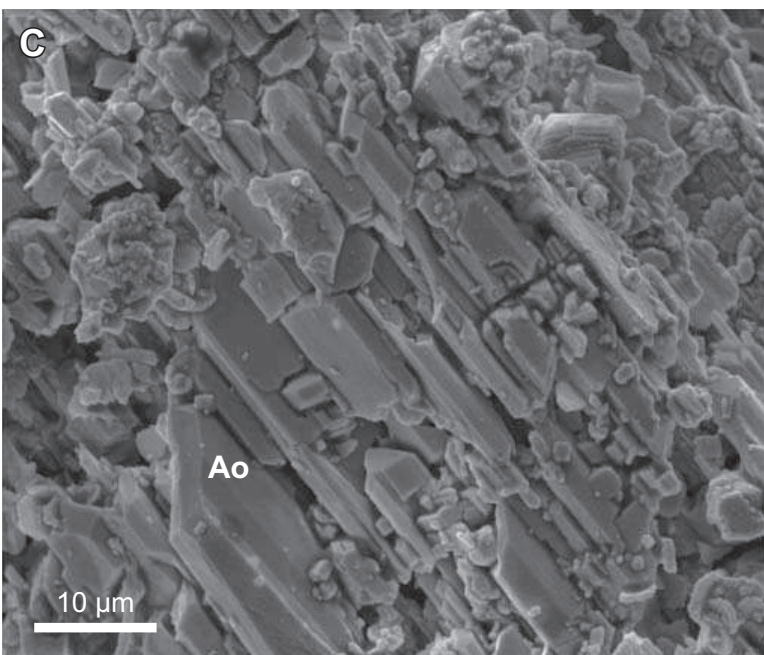
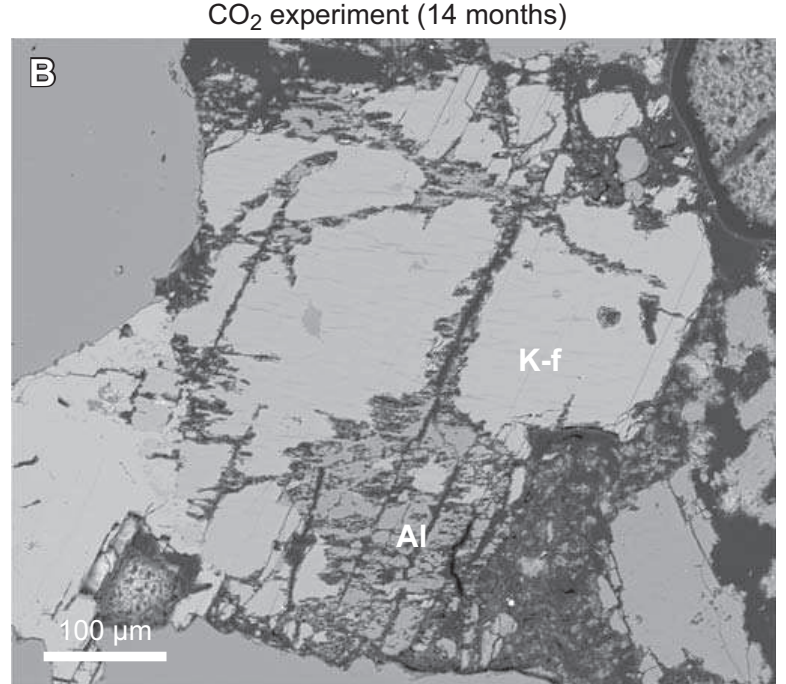
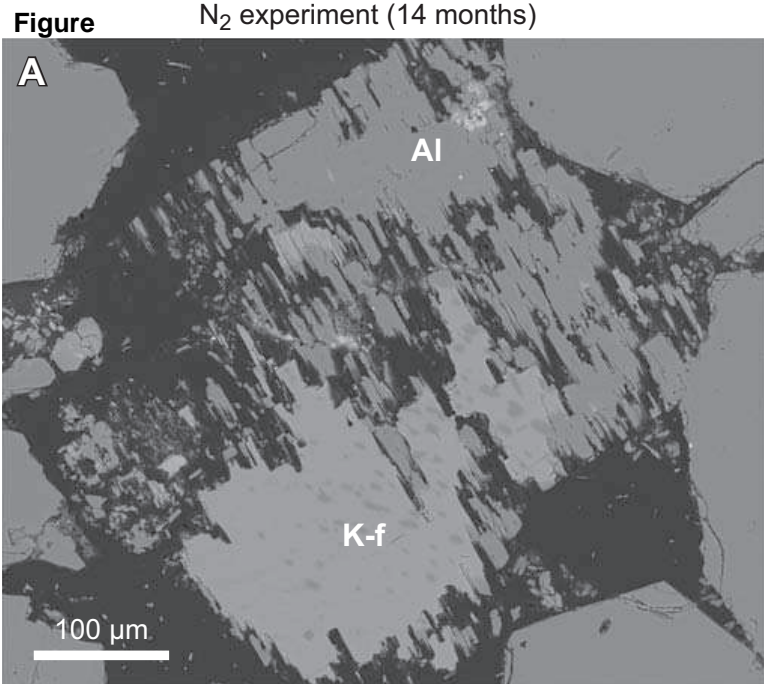


Figure

N₂ experiment (14 months)

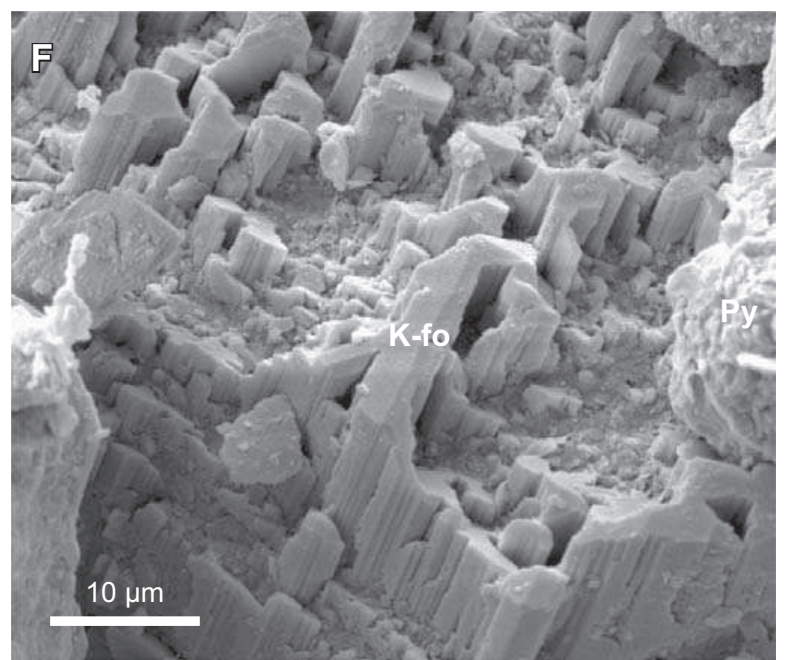
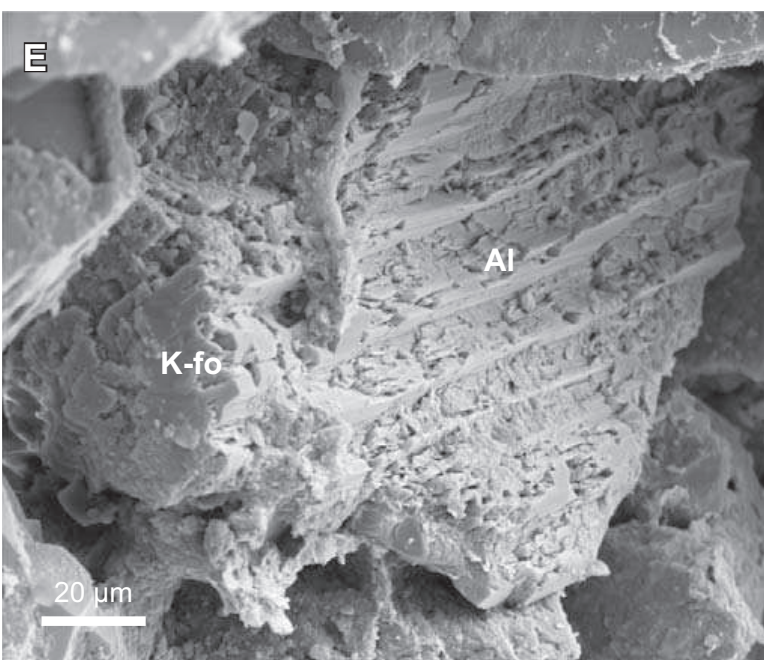
CO₂ experiment (14 months)





Prior to experiment

CO₂ experiment (14 months)



Figure

